The genetic control of rapid genome content divergence in *Arabidopsis thaliana*

Christopher J. Fiscus[1] and Daniel Koenig[1,2*]

[1] Department of Botany and Plant Sciences, University of California, Riverside, California, United States of America

[2] Institute for Integrative Genome Biology, University of California, Riverside, California, United States of America

* Corresponding author:
E-mail: dkoenig@ucr.edu (DK)

Abstract

Genome evolution in eukaryotes is predominantly driven by the dynamics of repetitive sequences, which vary widely in both copy number and sequence composition. The rate of repeat evolution changes between species and within a species and is likely modulated by both genetics and environment. To uncover the factors shaping the rate of genome content evolution, we analyzed 1,142 resequenced *Arabidopsis thaliana* genomes using a novel K-mer based approach. With this dataset, we characterized genome content variation and identified hypervariable regions that contribute to major differences in repeat abundance. We then treated repeat abundance as a quantitative trait and performed genome-wide association studies to map the genetic basis of copy number variation across more than 400 repeat families. We jointly analyzed these results using a meta-GWAS approach, revealing both cis-acting variants and over 50 trans-acting loci that regulate repeat abundance genome-wide. Finally, we found that purifying selection acts against mutations that increase the rate of genome content divergence, favoring alleles that limit repeat expansion. Together, our results provide new insights into the genetic architecture and evolutionary forces shaping genome evolution in plants.

Introduction

Although core biological processes have been largely conserved across the tree of life, genome content and size vary dramatically, even between closely related species (Gregory, 2001). For instance, in eukaryotes, the number of genes per genome ranges from a few (Corradi et al., 2010) to tens of thousands, and genome size ranges several orders of magnitude (Elliott and

Gregory, 2015). The lack of correlation between genome size and organismal complexity, called the “C value enigma” (Gregory, 2001), was a longstanding conundrum that was solved with the discovery of substantial interspecific variation in non-coding DNA (Stephan, 1989). Measurement of genome content by DNA hybridization methods (Britten et al., 1974; Britten and Kohne, 1968), and ultimately through the production of high-quality genome assemblies (Adams et al., 2000; Arabidopsis Genome Initiative, 2000; Lander et al., 2001) revealed that upwards of 90% of eukaryotic genomes consist of repetitive sequences (Mehrotra and Goyal, 2014). Originally thought to be non-functional junk (Ohno, 1972), it is now generally recognized that repetitive sequences can be functional. For instance, telomeres play a crucial role in protecting the ends of chromosomes from degradation (Chakravarti et al., 2021) and centromeric satellite repeats play a role in kinetochore assembly during meiosis and mitosis (Talbert and Henikoff, 2022). Repetitive sequences can also have profound effects on phenotype by directly modifying gene expression and alternating local genetic and epigenetic mutation rates (Le et al., 2015; Slotkin and Martienssen, 2007). Additionally, variation in repetitive sequence appears to be a major driver of genome content and size variation both over long (Novák et al., 2020) and short evolutionary timescales (Bosco et al., 2007).

The model plant *Arabidopsis thaliana* has a compact ~150 Mbp genome (Davison et al., 2007) with over 10% variation in genome content between accessions (Long et al., 2013). Compared to its closest ancestor *A. lyrata*, from which it diverged < 6 million years (Hohmann et al., 2015; Novikova et al., 2016), the *A. thaliana* genome is repeat poor, with the majority of repetitive sequences occupying the centromere and pericentromere (de la Chaux et al., 2012; Hu et al., 2011). Population-level surveys of structural variation (Göktay et al., 2020; Lian et al., 2024), as well as repeat (Baduel et al., 2021; Davison et al., 2007; Lian et al., 2024; Long et al.,

2013; Quadrana et al., 2016) and gene copy number variation (Lian et al., 2024; Zmienko et al., 2020), have previously been conducted in this system. Copy number variation and large indels in *A. thaliana* cluster in the repetitive sequences, often in the pericentromere, and more sequence losses are found than gains (Long et al., 2013). The majority of CNVs and indels overlap with transposable elements which are clustered in these regions. However, total TE content is relatively similar across sequenced accessions (Baduel et al., 2021). Instead the copy number of highly repetitive sequences in rDNA clusters and in the centromeres are reported to make up a substantial portion of intraspecific variation in genome size and content (Long et al., 2013).

Efforts to catalog sequence differences segregating between individuals have historically relied upon variant calling and coverage-based approaches in which high-throughput sequencing reads from diverse individuals are mapped to a single reference genome. The strength of variant calling pipelines is their ability to detect small changes in conserved sequences, but variation in sequences absent from the reference genome are inaccessible to this method. For example, a study of genome variation in *A. thaliana* identified sequences up to 9 Mbp in length present in individual genomes but missing from the *Col-0* reference genome (Long et al., 2013). Alternatively, coverage-based approaches have been used to estimate copy number variation of genes and repeats. Repetitive sequences are largely missing or collapsed into single sequences in many first generation reference genomes (Treangen and Salzberg, 2011), and may be found in various sequencing contexts, hindering their detection by coverage differences. While recent advances in sequencing and assembly have ushered us into an era of “telomere-to-telomere” genome assemblies (Nurk et al., 2022) and bountiful pan-genomes (Cochetel et al., 2023; Golicz et al., 2016; Gordon et al., 2017; Lian

et al., 2024; Liu et al., 2020; Montenegro et al., 2017; Zhao et al., 2018), the production and comparison of large numbers of genome assemblies remains cost prohibitive and technically challenging for many species. As such, the genomics community is investing substantially in developing methods to simultaneously compare very large numbers of eukaryotic genomes (Armstrong et al., 2020; Song et al., 2022; Zhou et al., 2024).

To complement variant calling and coverage-based approaches, we developed a K-mer based method to detect differences in genome content between individual genomes. K-mers are short sequences of length K that can be rapidly identified and counted in sequencing reads without the need for a genome assembly or alignment. K-mer profiles have been regularly used to compare and group genomes (Sievers et al., 2017). For instance, differences in K-mer profile have been used successfully to compare genomes in other systems such as maize (Liu et al., 2017) and *Drosophila* (Wei et al., 2014). Additionally, K-mer content has been used to estimate telomere length (Choi et al., 2021), estimate genome size variation (Sun et al., 2018) and as genotypes in GWAS in *A. thaliana* (Voichek and Weigel, 2020). Here, we first describe the development of our method before using it to catalog genome content variation in over 1,000 sequenced accessions of *A. thaliana*, focusing on copy number variation of repetitive sequences. We then mapped the genetic basis of repeat copy number variation for individual repeat families and used a “meta-GWAS” approach to identify trans-acting alleles affecting genome content variation more generally. Finally, we explore the evolutionary dynamics of associated variants and provide evidence that these variants appear to be under selection.

Results

Using K-mer profiles to characterize genome content with high-throughput sequencing data

We set out to characterize genomic variation in *A. thaliana*, with the goal of understanding which sequences vary in copy number between individuals. For this purpose, we explored using K-mer abundances in short read datasets to describe the content of a sampled genome, which we termed a genome content profile (GCP). We then used the genome content profiles to directly compare samples or to derive sequence copy number estimates for specific sequences of interest.

The first step in developing the method was to decide on the length of K-mer to use when generating the GCPs. Higher values of K make it easier to match sequences to their origin, but each increase in K grows the size of the dataset exponentially. As such, our priority was to identify the minimum value of K that could discriminate abundances of specific genomic sequences.

We started by comparing K-mer spectra in both repetitive and non-repetitive sequences in the *A. thaliana* reference genome for all values of K from 5 to 20. We reasoned that K-mers derived from repetitive sequences should be observed at a higher abundance than K-mers derived from non-repetitive sequences, if the length of K-mer was sufficiently large to discriminate between the two sequence types. We assessed when this condition was met by calculating the median abundance among the K-mers observed in each sequence bin (Fig 1A). The minimum value of K required to discriminate the increased abundance of repetitive sequences was 12.

We next explored whether changes in sequence copy number in the *A. thaliana* genome might be detected using 12-mer abundances. We simulated copy number variation of 1 KB sequences in the reference genome and compared the known copy number with 12-mer copy number estimates. The median R^2 between the simulated copy number changes and 12-mer based copy number estimates among 1,000 replicates was 0.98 (Fig 1B, Fig S1). We further validated this approach using published transposon abundances in the *A. thaliana* reference genome assembly (Cheng et al., 2017). We found 12-mer and annotation-based copy number estimates to be significantly associated in this dataset (Fig 1C, $R^2 = 0.53$, $p < 2.2 \times 10^{-16}$).

Finally, we validated that 12-mer abundances in real and simulated Illumina sequencing reads (~44X average genomic coverage) were strongly correlated with those in the reference genome assembly (Fig 1D, $R^2 = 0.86$, Fig S2). However, the correlation between Illumina derived and simulated K-mer abundances are reduced when Illumina reads are downsampled to coverages less than 5X and break down at coverages less than 1X (Fig S3). Thus, we concluded that moderate coverage whole genome sequencing datasets are appropriate for our method.

A pipeline to generate genome content profiles for hundreds of genomes

To apply our approach to characterize genomic diversity in *A. thaliana*, we built a pipeline to assay genome content using K-mer abundances derived from large high-throughput sequencing datasets (Fig S4). Raw sequencing reads were first processed and filtered to remove sequencing adapters, poor quality reads, and to correct likely base call errors. The filtered and processed reads were then mapped to the organellar genomes to filter reads likely

153 originating from these sequences. 12-mer abundances were then counted in the unmapped
154 reads. Finally, the 12-mer abundances for each sample were normalized for both GC content
155 and coverage differences across samples. The normalized 12-mer counts were then used to
156 estimate the abundance of sequences of interest for each sample based on the median
157 abundance of constitutive 12-mers for that sequence (Materials and Methods).

158 We then applied our pipeline to profile the genomes of 1,319 resequenced *A. thaliana*
159 collected from across the extant species range (1001 Genomes Consortium, 2016; Durvasula
160 et al., 2017; Zou et al., 2017) (Table S1). To ensure that the analyzed dataset was high quality,
161 we filtered samples that had low mappability, low coverage, extremes in %GC, or strong
162 correlation between %GC and 12-mer abundance (Fig S5). We further ensured that our dataset
163 reflected the genomic variation in *A. thaliana* with minimal redundancy by clustering the
164 individuals by genetic similarity and retaining one individual from each similarity group (static
165 tree cut threshold of 100,000 corresponded to differences at ~0.4% sites) for subsequent
166 analysis. In addition to normalization to reduce the variation in GC content and coverage
167 between samples (Fig S6-S7), we fit a linear model to control for the effect of sequencing
168 center bias, which we identified as a major factor driving variation in 12-mer abundance
169 between individuals (Fig S8). The final dataset represented 1,043 individual *A. thaliana*
170 genomes with the normalized abundances of 8,390,656 discrete 12-mers. We hence refer to
171 the normalized 12-mer abundances for each sample as a genome content profile (GCP).
172

173 Regional copy number variation across the *A. thaliana* genome

174 One feature of the GCPs is that they are inherently reference-free. Therefore, to determine
175 which regions of the *A. thaliana* genome contain the types of sequences that are variable

176 between accessions, we segmented the reference genome into 100 KB non-overlapping
177 windows and estimated the copy number variability of each window using the GCPs. For highly
178 repetitive sequences this does not necessarily mean that the specific copy number variation
179 occurs within that window, but it does indicate where the repeats that are most variable
180 genome-wide occur. Copy number variability is herein described using the standardized range
181 statistic (sR), which is defined as the range divided by the median of sequence abundance
182 across individuals.

183 Copy number variability per genomic window, as measured by sR, spanned over two
184 orders of magnitude (Fig 2A). In general, sR had a strong positive correlation with the
185 proportion of repetitive sequence within a window (Spearman's $\rho = 0.76$, $p < 2.2 \times 10^{-16}$, Fig
186 S9) and a strong negative correlation with the proportion of genic sequence within a window
187 (Spearman's $\rho = -0.79$, $p < 2.2 \times 10^{-16}$). Regions with the highest extremes of sR almost
188 exclusively corresponded to known cytological features including the pericentromere and
189 centromere on all five chromosomes, the nucleolar organizer region (rDNA) on chromosome 2
190 (NOR4 is missing from the reference genome), and the heterochromatic knobs on
191 chromosomes 4 (hk4S) and 5 (hk5L). In addition to heterochromatic regions of the genome,
192 highly variable regions included a cluster of pre-tRNA genes on chromosome 1, clusters of
193 cysteine-rich repeat secretory genes on chromosomes 3 and 4, and the RPP5 NBS-LRR
194 disease resistance gene cluster on chromosome 4. These data are consistent with previous
195 observations that some of these gene clusters show copy number variation between *A.*
196 *thaliana* accessions (Choi et al., 2016; Zmienko et al., 2020).
197

Copy number variation of representative repetitive sequences

To determine which specific sequences vary between accessions, we next estimated the copy number of annotated sequences of interest in each genome using the GCPs (Table S2). We cataloged copy number variation of known repetitive sequences and of universal single copy orthologous genes (BUSCOs). We expected that BUSCOs would have lower rates of CNV than repetitive sequences based on their long-term intraspecific retention as single copy genes. Copy number variability per representative repeat sequence, as measured by sR, ranged nearly 4 orders of magnitude (0.07 to 500) compared to ~1 order of magnitude for BUSCOs (0.08 to 0.69) (Fig S10). On average, DNA transposons had higher sR than retrotransposons and satellites and simple repeats had higher sR than transposons (Wilcoxon-Mann Whitney U test, Bonferroni adjusted $p < 0.05$).

We next identified repetitive sequences with strong changes in abundance over evolutionary time. We calculated a z-score for each repeat in each genome using the distribution of each repeat's estimated abundance across accessions. Outlier z-scores ($|z| > 3$; $p < .0027$) represent repeats with unusually high or low estimated abundances in an accession (Fig 2B). By this criteria, 98.6% of the tested repeats (648/657) changed in abundance in at least one accession, with an average of ~11 accessions showing a change for any particular repeat (Table S2). Changes in repeat abundance were strongly enriched for expansions rather than deletions (6,050 increases and 914 decreases). Of the 657 representative repeat sequences, 348 exhibited only increases in abundance relative to the population mean. These included 195 retrotransposons, 52 DNA transposons, 12 satellite sequences, and 88 simple repeats, including all dinucleotide repeats. A total of 289 repeat families showed both increases and decreases in abundance, with a median ratio of increases to decreases of 3. This group

comprised 137 retrotransposons sequences, 112 DNA transposon sequences (including all sequences from the mariner/Tc1 and pogo families), 8 satellite sequences, and 31 simple repeats. Only 11 repeat families exhibited decreases in abundance alone, including 8 retrotransposon sequences, the VANDALNX1 DNA transposon, and two satellite sequences (COLAR12 and the 5S rDNA repeat). An additional 11 repeat families showed no Z-score outliers, including 7 Copia superfamily elements, the L1 superfamily element TA11, the DNA transposon VANDAL18, and two hexamer repeats (Fig S11-S14).

The evolution of repeat expansion and contraction in *A. thaliana*

We next investigated variation in repeat content across the 12 major subpopulations of *A. thaliana* previously defined using SNP data (1001 Genomes Consortium, 2016; Durvasula et al., 2017; Zou et al., 2017). Principal component analysis (PCA) revealed subtle shifts in repeat content across subpopulations along the first principal component (PC1; Fig 3A). Loadings along PC1 indicated that these shifts were driven by copy number divergence across numerous repetitive sequences spanning all four major repeat classes (Fig. S15). Notably, DNA transposons showed particularly skewed loadings across multiple superfamilies, suggesting a disproportionate contribution to population-wide variation in repeat content (Fig S16).

To assess whether repeat content reflects subpopulation structure, we tested for clustering by subpopulation. Repeat abundance estimates significantly clustered individuals in six of the twelve subpopulations–North Sweden, Italy Balkan Caucasus, Central Europe, Asia, Africa, and China–more often than expected by chance (permutation test, 10,000 permutations; Bonferroni-corrected $p < 0.05$). In contrast, we found no significant clustering for Western Europe, South Sweden, Germany, Relict, Admixed, or Spain. Despite limited clustering at the

subpopulation level, the dominant pattern in the dataset was evidence of rapid, individual-level expansions and contractions of repetitive sequences (Fig. 3B). Consistent with this, the top 25 most divergent genomes were distributed across seven different subpopulations (Fig S17).

Although global patterns of repeat content clustered significantly in only half of the subpopulations, we observed numerous instances of copy number changes that were significantly enriched within individual subpopulation groups. In total, 252 distinct sequences showed significant enrichment for copy number variation across 12 admixture groups (Fisher's Exact test, Bonferroni-corrected p value across groups < 0.05, Table S3). South Sweden had the highest number of enriched sequences (N=138), followed by Asia (N=36) and Spain (N=22). In South Sweden, 135 sequences were enriched for copy number increases, including 78 DNA transposons, 17 retrotransposons, 4 satellites, and 36 simple repeats. This group also showed enrichment for copy number decreases in the 18S and 45S rDNA satellites and the ATMU8 MuDR superfamily DNA transposon. In Asia, copy number increases were enriched in 20 DNA transposons, 10 retrotransposons, 3 satellites, and 1 simple repeat, alongside a decrease in the ATCOPIA18A retrotransposon. Spain showed enrichment for copy number increases in 1 DNA transposon, 17 retrotransposons, and 2 simple repeats. The remaining groups had between 16 (Relict) and 2 (Admixed) sequences enriched for copy number change.

The genetic basis of repeat copy number variation

Our analyses suggest that genome content variation primarily arises through changes in repeat-dense, heterochromatic compartments of the genome. Differences in repeat abundance between subpopulation groups are generally subtle, with a small subset of accessions distributed across groups exhibiting extreme genome content divergence. One possible

267 explanation for this pattern is that these accessions may have accumulated one or more
268 mutations that affect the likelihood of CNV occuring. To investigate this hypothesis, we treated
269 the relative abundance of each repeat family as a quantitative trait and used a genome-wide
270 association study (GWAS) approach to identify loci associated with repeat copy number. We
271 tested 1,325,632 biallelic SNPs for association across 429 sequences, including 174
272 retrotransposons, 112 DNA transposons, all 22 satellites, and 121 simple repeats. In total,
273 29,891 SNPs were associated across 384 GWAS, including 142 retrotransposons, 58 DNA
274 transposons, 21 satellites, and 58 simple repeats (Table S4).
275

276 Pericentromeric regions are associated with repeat copy number
277 variation

278 To identify genomic loci associated with repeat copy number variation, we first examined the
279 genomic distribution of significant SNPs across all GWAS results (Fig 4A). Significant
280 associations were broadly distributed throughout the genome, with 94% of 100 KB windows
281 (1,122 of 1,193) containing at least one significant SNP, and a median of 13 significant SNPs
282 per window. This genome-wide pattern of significant SNPs was largely consistent across
283 repeat classes. Despite the broad distribution, significant SNPs were enriched in
284 pericentromeric regions, occurring more frequently than expected by chance (Fisher's Exact
285 Test, odds ratio 4.508, $p < 2.2 \times 10^{-16}$, Fig 4B).
286 Significant associations detected in our analysis may reflect either SNPs linked to copy
287 number variants themselves (which we refer to as *cis*-acting associations) or SNPs linked to
288 mutations that alter the rate that CNVs arise (i.e., putative *trans* mutators). Since repetitive
289 sequences are concentrated within the pericentromeric and centromeric regions of *A. thaliana*

290 (Fig 2A, (Quesneville, 2020)), we hypothesized that the observed enrichment of significant
291 SNPs in these regions likely reflects *cis*-acting variation in repeat copy number. To test this, we
292 identified GWAS with enrichment for significant SNPs in the pericentromere, restricting our
293 analysis to the 291 repeat families with at least 10 significant SNPs. We found significant
294 pericentromeric enrichment in GWAS for copy number variation in 76 of 138 retrotransposons,
295 19 of 90 DNA transposons, 15 of 21 satellites, and 14 of 42 simple repeats (Fisher's Exact Test,
296 Bonferroni-corrected $p < 0.05$, Table S2). Of the retrotransposons tested, 45% (35 of 77) of
297 Copia superfamily elements and 75% (40 of 53) of Gypsy superfamily elements showed
298 significant enrichment of SNPs in the pericentromere. Similarly, all DNA transposons from the
299 En/Spm superfamily, except ATENSPM1, were enriched in the pericentromere, along with
300 ATHAT1 of the hAT superfamily, 41% (11 of 27) MuDR elements and 43% (3 of 7) VANDAL
301 superfamily elements. In contrast, we detected no pericentromeric enrichment in GWAS for
302 retrotransposons of the L1 or SADHU superfamilies or DNA transposons from the Helitron,
303 mariner/Tc1, and pogo superfamilies. All satellites save for rDNA repeats and ATCLUST1 were
304 enriched for centromeric SNPs. The GATCGATCGATC tetramer and some penta- and hexa-
305 mers were also enriched for significant SNPs in the pericentromere. Supporting the
306 interpretation that these associations reflect *cis*-linked CNVs, repeats with pericentromeric
307 enrichment in GWAS were significantly more common in pericentromeric regions than in
308 chromosome arms (Fisher's Exact Test, odds ratio 10.349, $p < 2.2e-16$, Fig S18).
309 Changes in pericentromeric repetitive sequences were not distributed evenly across the
310 five pericentromeres (Table S5). In general, for transposons, there was a mixture of Copia and
311 Gypsy superfamily LTR retrotransposons localized to all five pericentromeres, VANDAL
312 superfamily DNA transposons localized to the pericentromeres on chromosomes 1-3, MuDR

superfamily DNA transposons localized to the pericentromeres in chromosomes 2-5, and En/Spm superfamily DNA transposons localized to the pericentromeres on chromosomes 1-2. Notable sequences with sequence abundance variation localized to pericentromere 1 included a number of Copia transposons including ONSEN (ATCOPIA78), Gypsy transposons of the ATHILA8A family, satellite ATREP18 which contains the major telomere repeat, and centromere satellite variants from clusters 5 and 6. We localized abundance variation in AtSB5, a SINE non-LTR retrotransposon, and ATMSAT1, a mini- satellite, to the pericentromere on chromosome 2. Of note localized to pericentromere on chromosome 3 were all families of autonomous ARNOLD MuDR superfamily DNA transposons, and centromere satellite variant AR3. Pericentromere 4 was marked with variation in abundance of ATHAT1, the only hAT superfamily DNA transposon localized to a pericentromere, and numerous centromere satellite variants (AT12, COLAR12, cluster 2, cluster 3), as well as the major knob repeat of hk4S (ATENSAT1). Aside from transposons described previously, the only notable sequences localized to pericentromere 5 were variants of the hk5L knob repeat.

Taken together, our results suggest that much of the repeat copy number variation in *A. thaliana* can be attributed to variation linked to pericentromeres.

Trans-acting regulators of repeat copy number variation

We took two related approaches to identify *trans*-acting loci that may affect the abundance of several repeats simultaneously. First, we conducted a meta-GWAS analysis using our association studies of the abundances of 207 sequences consisting of 104 retrotransposons, 34 DNA transposons, and 69 simple repeats. Second, we used the first axis of a PCA of repeat abundances as a trait in another genome-wide association study.

336 A large number of candidate *trans*-acting loci were revealed using these two
337 approaches. The meta-GWAS yielded 228 significant SNPs, which were collapsed into 57
338 discrete peaks after pruning for linkage disequilibrium (Fig 5A, Table S6). GWAS on PC 1
339 yielded 84 significant SNPs, sharing 65 significant SNPs and 19 peaks with the meta-GWAS
340 (Fig 5B). The congruence of these analyses suggests that this approach captures loci generally
341 associated with variation in repeat content between *A. thaliana* genomes.
342 Gene ontology enrichment analysis (GO analysis) for biological processes enriched in
343 genes under meta-GWAS peaks yielded 63 significant GO terms at $p < 0.05$ (Table S7).
344 Associated GO terms were involved in several biological processes including response to biotic
345 and abiotic stresses (e.g. defense response to oomycetes, regulation of systemic acquired
346 resistance, negative and positive regulation of plant-type hypersensitive response, and
347 response to photooxidative stress), plant development (e.g. root development, floral whorl
348 development, and maintenance of seed dormancy by abscisic acid), and DNA replication and
349 repair (e.g. DNA repair, premeiotic DNA replication, and mitotic recombination-dependent
350 replication fork processing). The latter of these enrichments suggested that changes near
351 genes involved in DNA repair may be associated with genome divergence *A. thaliana*.
352 We subsequently manually examined the meta-GWAS peaks to identify potential
353 candidate genes with activity linked to repeat copy number variation. Consistent with the
354 results of the GO analysis, we found more than a dozen genes involved in DNA replication
355 and/or DNA repair pathways underlying the peaks (Table S6). In total, we identified candidate
356 loci for 21 of the peaks, with 9 tag SNPs predicted to be missense variants or linked to
357 predicted missense variants ($R^2 > 0.20$). We hereafter identify genes tagging putative missense
358 variation with an "*".

359 Candidate genes involved in DNA replication included *ORC6** (AT1G26840), a subunit of
360 the DNA replication origin recognition complex (Masuda et al., 2004), *PCNA1* (AT1G07370), a
361 sliding clamp that acts in leading strand elongation (Strzalka and Ziemienowicz, 2011), and
362 *PROLIFERA* (AT4G02060), a component of the minichromosome maintenance complex
363 (Springer et al., 2000).

364 Candidate genes with a role in DNA repair were mostly active in the repair of DNA
365 double strand breaks via homologous recombination. Examples include *HIGLE* (AT2G30350), a
366 SLX1 family endonuclease that resolves Holliday junctions (Verma et al., 2022), *FANCD2**
367 (AT4G14970) a homolog of Fanconi anemia D2 that is essential for homologous recombination
368 during meiosis (Kurzbauer et al., 2018), the homolog of *RAD51* (AT5G20850) (Doutriaux et al.,
369 1998), involved in homology search during homologous recombination (Li et al., 2004), and the
370 homolog of breast cancer susceptibility gene 2 (*BRCA2B*, AT5G01630) which recruits *RAD51*
371 and *DMC1* during double-strand break repair via homologous recombination (Seeliger et al.,
372 2012). Additional candidates involved in DNA double strand break repair included *XRCC4**
373 (AT1G61410), a homolog of a DNA ligase IV binding protein with a role in the non-homologous
374 end joining pathway (West et al., 2000) and DNA polymerase gamma-2 (*POLGAMMA2*,
375 AT1G50840), an error-prone organellar DNA polymerase encoded in the nucleus (Ayala-García
376 et al., 2018).

377 Candidate genes implicated in the repair of other classes of DNA damage were also
378 observed under meta-GWAS peaks. Examples include MutM homolog *MMH-1** (AT1G52500),
379 which is involved in the repair of single strand nicks due to oxidative DNA damage during base
380 excision repair (Ohtsubo et al., 1998) and *CHC1* (AT5G14170), a subunit of SWI/SNF chromatin
381 remodeling complex involved in repair of DNA damaged by UV-B (Campi et al., 2012). We also

382 found *SNI1** (AT4G18470), a subunit of the Smc5/6 complex that reacts to DNA damage by
383 acting as a DNA micro-compaction machine that identifies unusual DNA conformations
384 (Serrano et al., 2020).

385 In addition to genes involved in DNA repair, we found many candidates with roles in
386 DNA methylation and DNA demethylation, which likely act in the epigenetic regulation of
387 repetitive sequence proliferation. Notable candidates involved in DNA methylation included
388 *CMT3* (AT1G69770), a plant-specific chromomethylase which methylates cytosine at non-CpG
389 sites (Lindroth et al., 2001) and *RRM1** (AT3G54760), which interacts with *SUVH9* to regulate
390 RNA-directed DNA methylation (Zhou et al., 2021). Candidates acting in DNA demethylation
391 included *DML1/ROS1** (AT2G36490), which demethylates DNA (thus repressing gene silencing)
392 (Gong et al., 2002) and *MEM1* (AT1G48950), which removes CHH methylation (Lu et al., 2020).
393 Further candidates included *NRPE3B** (AT2G15400), a subunit of plant-specific RNA
394 polymerase V with a role in siRNA-directed DNA methylation (Ream et al., 2009), *ABCE2*
395 (AT4G19210), a RNase L inhibitor that suppresses RNA silencing (Braz et al., 2004), and *RPS6*
396 (AT4G31700) a component of the 40S ribosomal subunit that represses rDNA transcription (Kim
397 et al., 2014).

398 We examined the extent that the 57 loci identified in the meta-GWAS were significant in
399 individual GWAS for repeat copy number change. In total, 53 loci were significant in one or
400 more GWAS, with 12 associated with GWAS in all four repeat classes, 16 found in three repeat
401 classes, 14 found in 2 repeat classes, and 11 found in only one repeat class (Fig. 5C, Table S4).
402 Four loci were significant in the meta-GWAS but were not significant in any individual sequence
403 copy number GWAS nor in the PC 1 GWAS. The former loci included the peaks with
404 candidates *SNI1* and *NRPE3B* as well as two loci without an identified candidate.

To understand whether associated peaks have consistent effects on different repeat classes we characterized the effect of the minor allele on sequence copy number among the individual GWAS for each peak. The majority of loci promote copy number variation across different repeats in the same direction (66%, 26 increasing and 9 decreasing abundance, Fig. 5C). Among the peaks with mixed effects, 5 peaks have mixed effects in two or more classes and 3 have mixed effects in one class only. These data indicate that most of the putative mutator alleles that we have identified in *A. thaliana* generate mutations that are more likely to increase copy number. How these loci are generating directional shifts in repeat copy number remains to be explored.

Evolutionary dynamics of putative mutator alleles

Finally, we calculated the species-wide site frequency spectrum to assess whether loci associated with repeat copy number variation are subject to selection. We observed a significant enrichment for rare alleles (minor allele frequency < 0.10) among both meta-GWAS tag SNPs and SNPs significant in one or more GWAS, relative to nonsynonymous SNPs (Fig. 6A, Chi-squared tests, $p = 0.031$ and $p < 2.2 \times 10^{-16}$, respectively). However, there was no significant enrichment of rare SNPs in the meta-GWAS tag SNPs when compared to putatively causative SNPs from the AraGWAS database (Togninalli et al., 2020, 2018), even when stratifying meta-GWAS SNPs by the direction of derived allele effect. Our results suggest that variation associated with repeat copy number change is likely under purifying selection, as indicated by the excess of low-frequency alleles.

If purifying selection is acting to purge mutations that drive rapid genome content divergence, then the strength of selection within a population should influence the rate of

genome evolution. We found that many of the accessions with evidence of rapid genomic divergence occur outside of the core of the species' European range, where effective population sizes are smaller. To test whether repeat differences between populations could be attributed to variation in the strength of selection, we examined the relationship between the number of sequences with copy number changes per group and the strength of genetic drift, estimated by the ratio of derived allele frequencies between nonsynonymous and synonymous variants (Fig 6B). We observed a strong positive correlation Spearman's $\rho = 0.76$, $p = 0.02$) between these parameters, suggesting that populations with more extensive copy number changes have likely experienced relaxed selection.

Discussion

A K-mer based method to estimate sequence copy number

Here, we present a novel K-mer based approach to estimate sequence copy number from high-throughput sequencing reads and apply the method to study genome content variation in a species-wide survey of wild *A. thaliana.* The method is designed to profile genomes sequenced with short read technology while avoiding the complexities of genome assembly. As such, the method is useful to study sequences that present difficulties for genome assembly such as repetitive sequences (Treangen and Salzberg, 2011), but it has the disadvantage of being unable to localize a sequence in a genome. While we have entered the era of complete (i.e. telomere-to-telomere) genome assemblies (Nurk et al., 2022), such assemblies take considerable resources to produce and will likely be infeasible for studying genomic variation at population scale for some time. In contrast, our method does not require high-coverage

450 sequencing or long reads and thus represents a cost-effective method to study genomic
451 variation in many samples. Our method can also be readily applicable to the extensive library of
452 high-throughput sequencing reads in public databases such as NCBI SRA.

453 One important consideration when running the pipeline is the choice of length of K-mer
454 to use. While we describe a method here to choose K and decided to use K = 12 for this work,
455 we admit that the choice of K is somewhat arbitrary and could affect the accuracy of the
456 sequence copy number estimates. While we had success in mapping variation in genome
457 content with K = 12, our K-mer based estimates of repeat abundance are imperfectly
458 correlated with annotated repeat abundance. We erred on the side of choosing a smaller K
459 since each increase in K increases the size of the dataset exponentially and increases the
460 number of uninformative singletons (i.e. K-mers with abundance 1). Future work with larger K
461 and simultaneous filtering of singleton K-mers to reduce the dataset size might provide more
462 accurate copy number estimates and increase the power of subsequent analyses.

463 We used the genome profiles generated by our pipeline to estimate sequence copy
464 number using the abundance of K-mers that constitute a focal sequence. This application is
465 dependent on providing reference sequences from which the K-mer hash table is derived. For
466 our work, we primarily focused on studying copy number variation in known repetitive
467 sequences previously identified in *A. thaliana* and contained within RepBase (Bao et al., 2015).
468 However, comprehensive repeat libraries are not yet available for the majority of systems. While
469 approaches to construct such libraries do exist (e.g. EDTA (Ou et al., 2019)), contemporary
470 approaches require high-quality genome assemblies with assembled repeats. Additionally, our
471 method imperfectly handles variation in the representative sequences. While the method is able
472 to handle sequences with variation coded by IUPAC nucleotide ambiguity codes, the current

implementation generates all possible K-mers encoded by the ambiguity code and then substitutes the median value of the possible K-mers for the ambiguous K-mer when calculating the abundance estimate. If there are multiple ambiguous nucleotides within a single K-mer, the number of K-mers considered can be quite large, costing performance. An improved implementation of the pipeline could substitute a weighting scheme to better handle conserved and variable sequences within a reference sequence.

A major issue with the approach is that K-mer profiles seem to be especially sensitive to technical biases in sequencing that are typically unaccounted for in genomic analyses. We discovered this effect by doing a principal component analysis of 12-mer profiles and realized that samples clustered according to the sequencing center (Figure S8). We investigated this issue by attempting to isolate the variable responsible for the technical bias. Specifically, we examined GC content differences between libraries, possibility of organellar genome contamination, and the effect of low and high abundance 12-mers on genome content profiles. Ultimately, we were unsuccessful in determining the cause of the bias. In particular, in the 1001 Genomes dataset, population group and sequencing center were confounded, making it impossible to distinguish between biological and technical variation. In the end, we dealt with this issue by fitting a linear model to coarsely remove the effect of sequencing center from genome content profiles, with the understanding that we were also likely removing some biological variation from the dataset. Our recommendation for further use is to avoid the issue of technical sequencing bias by sequencing replicate samples randomized across sequencing runs.

Genome content variation in wild *A. thaliana*

Our results suggest that genome divergence between *A. thaliana* accessions is largely explained by copy number variation of repetitive sequences in heterochromatic-rich regions of the genome such as the nucleolar organizing regions, pericentromeres, and centromeres. This is consistent with the observation of very high collinearity in gene-rich regions of 69 chromosome-scale *A. thaliana* genomes (Lian et al., 2024). The implication is that highly repetitive sequences are probably among the most rapidly evolving sequences within the genome and therefore could underlie genomic changes that eventually lead to speciation. Analysis of the genome of *A. lyrata*, the closest ancestor to *A. thaliana* found that the large difference in genome size between the two species (~70 Mbp) could be primarily attributed to the purging of transposable elements along with non-coding DNA in the lineage leading to *thaliana* (Hu et al., 2011) and comparison of centromere assemblies between the two species showed complete divergence of the orthologous centromeres (Wlodzimierz et al., 2023). Extensive sequence divergence has also been found in copies of the 178bp canonical major centromeric satellite repeat (*AthCEN178*) both within (Maheshwari et al., 2017) and between *A. thaliana* genomes, with almost a quarter of individual repeat copies unique to a specific genome (Wlodzimierz et al., 2023).

An alternative non-exclusive explanation for the divergence pattern is that purifying selection is much weaker in regions of the genome that are repeat-rich (and thus gene-poor). This view is supported by evidence that in general, TEs can insert all over the genome and seem to lack a preference for inserting within the repeat-rich pericentromeres and centromeres (Quadrana et al., 2016). Thus, TEs that insert near genes are rapidly purged by strong purifying selection (Hollister and Gaut, 2009), with selection pressure greater than that exerted on

518 missense SNPs (Baduel et al., 2021). Mechanianistially, the weakening of purifying selection in
519 repeat rich regions could be a local reduction in recombination rate in repeat-rich regions of the
520 genome. This is especially true of centromeres, which have been shown to have both low and
521 non-recombining compartments (Fernandes et al., 2024).

522 Overall, we observed many more instances of repeat copy number increase compared
523 to decrease. This pattern could be indicative of repeat expansions being more frequent than
524 contractions or due to stronger purifying selection against copy number decreases compared
525 to increases. Although our data does not allow us to discriminate between these two
526 possibilities, the enrichment for rare variants was stronger for alleles associated with copy
527 number decrease compared to increase (Fig. 6A), lending credence to the latter hypothesis.
528 The latter hypothesis is further supported by the observation that most transposons in the *A.*
529 *thaliana* genome appear to predate speciation (Quesneville, 2020), suggesting that deletions of
530 these sequences would be strongly deleterious. It remains to be seen whether stronger
531 selection against further deletions is the result of the already extensive genome reduction in *A.*
532 *thaliana* making further deletion more likely to disrupt biological function.

533 Our work has many similarities with a smaller survey of transposon copy number
534 variation in 211 accessions (Quadrana et al., 2016). Of the 174 transposon superfamilies
535 analyzed in both studies, the presence or absence of copy number variation was consistent
536 between the previous study and our work for 80 superfamilies. In contrast, we identified copy
537 number variation in 30 superfamilies not identified in the smaller cohort while they detected
538 CNV in 64 superfamilies which were not detected in our work. Despite these discrepancies, 24
539 of 59 comparable GWAS had one or more shared peaks between studies. It is unclear whether
540 coverage-based or K-mer based copy number estimates generated from sequencing reads are

more reliable indicators of transposon copy number variation between genomes. We anticipate that repeat analysis in chromosome-scale genome assemblies (Kang et al., 2023; Lian et al., 2024; Wlodzimierz et al., 2023) will clarify which families have copy number variation in *A.thaliana*.

The genetic basis of repeat copy number variation

In addition to mapping *cis*-acting repeat copy number variants, we identified over 50 distinct *trans*-acting loci regulating repeat copy number variation. These *trans*-acting loci were enriched for genes involved in DNA repair, DNA replication, and DNA methylation pathways. Notably, among the candidate genes associated with DNA repair, the majority function in the repair of DNA double-strand breaks (DSBs), which is consistent with the role of DSBs in promoting copy number variation through mechanisms such as transposon activity (Turlan and Chandler, 2000) and recombination events that underlie the expansions of simple repeats and satellites (Gadgil et al., 2020).

We also identified candidate genes involved in other DNA repair pathways, including nucleotide excision repair, which resolves intrastrand crosslinks and bulky adducts, and base-excision repair, which repairs single strand lesions. While these latter pathways may not directly mediate repeat amplification, they can repair collateral DNA damage associated with the proliferation of repetitive elements. For example, in the cut-and-paste replication of DNA transposons, transposase activity can introduce single-strand breaks at the donor site (Hickman and Dyda, 2015). Additionally, the DNA repair processes themselves can generate sequence copy number variation: single strand breaks are extremely common in plant

genomes (Wolter et al., 2021) and have been directly linked to the formation of tandem duplications of short repeats (Schiml et al., 2016).

Our work suggests that rapid changes in genome content arise sporadically throughout *A. thaliana*'s range, in part due to mutations that alter the efficiency of various DNA repair pathways and DNA methylation processes. Changes in genome content appear to be deleterious, as they are associated with rare genetic variants and occur more frequently in populations where purifying selection is less effective. We expect that both our ability to detect the effects of these mutations and the efficacy of selection in shaping their consequences are influenced by *A. thaliana*'s predominantly self fertilizing mating system. In outcrossing species, mutator loci are rapidly segregated away from the CNV that they induce. In contrast, a self fertilizing lineage that acquires one or more mutator alleles may be doomed to accumulating large numbers of deleterious CNVs unless rescued by an outcrossing event that allows mutators to be recombined away from their deleterious genomic consequences. Our ability to detect these lineages in *A. thaliana* suggest that they either occur at relatively high frequency, or persist for several generations.

Together, these data suggest a model in which mutator loci emerge in a self fertilizing lineage, induce elevated copy number variation rates, and persist when purifying selection is weak or the consequences of the specific genomic changes in content are small. If outcrossing occurs, progeny that do not carry the mutator loci could retain changes in genome content. Populations with small effective population size, where this cycle may occur more frequently, could be placed on a path of rapid genomic content evolution. This model may help explain the episodic bursts of repeat expansions that characterize genome content evolution across the plant kingdom.

Materials and Methods

Genome annotation

To identify repetitive and non-repetitive bins of the *A. thaliana* genome, we annotated the reference genome assembly (TAIR10) (Lamesch et al., 2012) with RepeatMasker 4.1.1 (Smit, AFA, Hubley, R & Green, P, 2013-2015) using the Dfam 3.2 library (Storer et al., 2021) and specifying "-species arabidopsis". Presumed conserved single copy genes were identified by annotating the reference genome with BUSCO 3.02 (Simão et al., 2015; Waterhouse et al., 2018) using the Eudicotyledons OrthoDB release 10 (Kriventseva et al., 2019) library. Augustus 3.3 (Stanke et al., 2008) was used as a dependency for the BUSCO pipeline.

K-mer analyses of TAIR10 reference genome

Canonical 5 - 20 mers were counted in repetitive and non-repetitive sequences of the *A. thaliana* reference genome using jellyfish 2.2.9 (Marçais and Kingsford, 2011). Designation of sequence as repetitive or non-repetitive was based on the RepeatMasker annotation described previously. From these K-mer counts, the number of unique K-mers and the median K-mer abundance per 100 Mbp bin were calculated.

To demonstrate that 12-mer profiles generated using the pipeline from sequencing reads reflect 12-mer profiles from genome assemblies, canonical 12-mers were calculated using jellyfish as described above for the reference genome and compared to normalized 12-mer counts produced by the software pipeline depicted in Figure 1A. A linear model was fit to log-transformed 12-mer counts using R (R Core Team, 2013).

To explore how coverage affects the relationship between the respective 12-mer profiles generated from sequencing reads and genome assemblies, Spearman's correlation was calculated between 12-mer profiles generated from Col-0 whole-genome sequencing reads (1001 Genomes Consortium, 2016) and the reference genome. For the sequencing reads, both empirical and simulated data were considered at coverages of 20, 10, 5, 2.5, 1, 0.5, 0.25, and 0.1X. Seqtk 1.2-r95 (Li, n.d.) was used for sampling of empirical data and wgsim 1.9 (Li et al., 2009) was used to simulate 100bp reads from the TAIR10 assembly.

Simulations

To demonstrate the accuracy of our pipeline that produces copy number estimates derived from 12-mer abundances in sequencing reads, we performed 1,000 simulations wherein directed copy number changes were introduced into the reference genome assembly, Illumina sequencing reads were simulated from the genome with introduced copy number variation, and the linear relationship between the copy number estimates produced by our pipeline (based on 12-mer abundances in sequencing reads) was compared to the actual relative copy number of a random 1KB sequence for -1 to +10 copies. For each simulation, we first simulated background polymorphism by generating 100 random copy number variations ranging from 100 to 10,000 bp with a max copy number of 10 and copy number variation gain loss ratio of 1 in the *A. thaliana* reference genome using simulG v1.0.0 (Yue and Liti, 2019). We then selected a random 1 KB sequence and simulated deletion (-1 copy) to +10 tandem insertions copies of the selected sequence using simulG. Single-end 100 bp Illumina HiSeq 2000 reads at 5X coverage were simulated from each genome with directed copy number change with ART_Illumina v2.5.8 (Huang et al., 2012). Canonical 12-mers were counted in the

simulated reads using jellyfish v2.2.9 (Marçais and Kingsford, 2011) and copy number estimates were produced using the last step of the pipeline depicted in Figure 1A. Linear models were fitted in R (R Core Team, 2013).

Genome content profiles

Sequencing reads from 1,319 previously sequenced accessions of *Arabidopsis thaliana* (studies PRJNA273563 (1001 Genomes Consortium, 2016), PRJEB19780 (Durvasula et al., 2017), and SRP062811 (Zou et al., 2017)) were downloaded from the European Nucleotide Archive. The reads were adapter and quality trimmed with Trimmomatic 0.36 (Bolger et al., 2014) to remove sequencing adapters, low quality sequence on read ends (quality < 20), low quality sequence in sliding windows (clip at quality < 20 in 4 bp sliding window), the first 20 base pairs of each read, and reads less than 36 base pairs long. A custom adapter file containing all Illumina single end (SE) or paired end (PE) adapter sequences was used to trim adapters from SE or PE reads, respectively. Trimmed reads were then error corrected with BayesHammer (Nikolenko et al., 2013) as implemented in SPAdes 3.15.0 (Bankevich et al., 2012) using the default parameters. Error-corrected reads were then mapped to both the reference genome and the organellar genomes (Arabidopsis Genome Initiative, 2000) separately with bwa 0.7.17 (Li, 2013; Li and Durbin, 2009). Alignment statistics were calculated with samtools 1.9 (Li et al., 2009). To reduce contamination from reads originating from the organellar genomes, reads that did not map to the organellar genomes were extracted from the alignments with bedtools 2.27.0 (Quinlan and Hall, 2010). Canonical 12 mers (i.e. sequences and reverse complements were binned together) were counted in the unaligned reads using jellyfish 2.2.9 (Marçais and Kingsford, 2011).

654 To remove samples that likely contained contamination, samples in which less than
655 90% of processed reads mapped to the reference genome were excluded from further
656 analysis. Samples with coverage less than 1X based on coverage estimates produced using
657 the sum of raw K-mer abundances found in the library divided by the approximate size of the
658 genome (150 Mbp) were also subsequently disqualified. To remove libraries with extremes of
659 GC content, which are likely due to PCR-bias during library preparation (Aird et al., 2011),
660 samples with extreme GC content were filtered according to the 1.5 IQR rule.

661 To enable the comparison of 12-mer profiles between accessions, 12-mer counts for
662 each sample were normalized according to a two step process. First, to correct for GC content
663 bias due to variable library preparation across samples, raw 12-mer counts were transformed
664 such that the proportion of counts that fell into GC bins defined by the GC content of each
665 12-mer sequence was constant across samples. As a “reference sample” for the
666 transformation, the proportion of counts attributed to each GC bin was calculated using the
667 median count for each 12-mer across accessions. For each sample, the proportion of counts
668 attributed to each GC bin was tabulated and a weight was calculated as the ratio of the
669 proportion of the “reference sample” counts in each GC bin to the proportion of the sample
670 counts in each GC bin. Sample counts were then transformed by multiplying the raw counts by
671 the corresponding weights of each GC bin. Samples with extreme Spearman’s correlation
672 between GC-normalized 12-mer count and 12-mer GC content were also filtered according to
673 the 1.5 IQR rule.

674 To normalize for coverage differences, GC transformed counts were normalized by
675 quantile-quantile normalization using limma v. 3.44.3 R package (Ritchie et al., 2015). To reduce

676 the impact of technical biases on 12-mer profiles, we removed the effect of the sequencing
677 center by fitting a linear model.
678 Finally, near-isogenic accessions were filtered from the dataset. Genetic distance was
679 calculated using published SNP genotypes (1001 Genomes Consortium, 2016) with plink 1.9
680 (Chang et al., 2015) and the distance matrix was hierarchically clustered and static tree cut at a
681 height of 100,000 in R (R Core Team, 2013). For each cluster defined by the tree cut, one
682 sample was randomly selected to be retained for further analysis and the remaining samples
683 were filtered.
684

685 Sequence abundance estimation with genome content
686 profiles

687 The abundance of annotated sequences were estimated in each genome content profile by
688 extracting the overlapping 12-mers that compose the feature and calculating the median count
689 of these representative 12-mers (Fig #). This value was then transformed to an abundance
690 estimate according to the following exponential equation: 2^x, where x is the median count of
691 representative 12-mers. For all sequences besides the genomic windows, the abundance
692 estimates were normalized by the median abundance estimate for complete single copy
693 BUSCO genes within each sample. The *A. thaliana* Repbase 23.10 library (Bao et al., 2015) was
694 used as the library of sequences for which copy number was estimated and supplemented
695 with a 5S rDNA sequence from GenBank (GenBank M65137.1), a 45S rDNA sequence
696 (Rabanal et al., 2017), and consensus sequences of each of the six 180bp centromere satellite
697 variants described by (Maheshwari et al., 2017). Consensus sequences for each of the

centromere satellite variant clusters was determined by further clustering sequences from each cluster with vsearch 2.9.1 (Rognes et al., 2016) with a 75% identity threshold. The centroid that represented the greatest number of sequences per cluster was then used as the representative sequence for that cluster.

Sequence abundance variability across accessions and groups

The standardized range (sR), defined as the range divided by the median of sequence abundance across accessions, was used to estimate sequence abundance variability.

To assess differences in repeat abundance across populations, we first calculated Z-scores for the normalized abundance estimates. We then applied hierarchical clustering to the resulting matrix, clustering both individuals (columns) and sequences (rows). To test the clustering of individuals within subpopulations or sequences by class, we used a permutation approach. Specifically, we compared the within-cluster sum of squares of observation ranks to 10,000 random shufflings of the categorical labels to generate an empirical p-value for each observation.

To identify sequences with enrichment for copy number increases or decreases per subpopulation, we asked whether there was an enrichment of individuals within a subpopulation with extreme scaled abundance estimates suggestive of copy number increase ($Z > 3$) or copy number decrease ($Z < 3$) compared to all other samples. Enrichment was calculated using Fisher's Exact test as implemented in the R stats package (R Core Team,

2023). P values were corrected for multiple testing using Bonferroni's method, with the number of tests corresponding to the number of groups for each sequence.

Variant filtering and genome-wide association

Published variant calls from the 1001 Genomes Project (1001 Genomes Consortium, 2016) were filtered with bcftools 1.8 (Li et al., 2009) and plink 1.9 (Chang et al., 2015) to retain biallelic sites called in 95% of individuals with a minimum minor allele frequency of 0.01 and minimum quality of 30.

Sequence abundance was treated as a molecular phenotype and mapped using genome-wide association with a mixed-linear model with GEMMA 0.98 (Zhou and Stephens, 2012). Only sequences with a sR greater than the 99th percentile of sR across BUSCO genes were included in the analysis. A centered relatedness matrix was used to correct for population structure. K-mer sequence abundance estimates were $\log_2$-transformed prior to analysis. Bonferroni threshold ($\alpha/N,\ where\ N\ is\ the\ number\ of\ variants$) was used to determine significant variants for individual studies.

To determine if significant SNPs were enriched in the pericentromere and centromere, one-sided Fisher's Exact tests were applied to 2 X 2 contingency tables describing whether SNPs were significant or not or found within the pericentromere and centromere or chromosome arms. Only GWAS with 10 or more significant SNPs were included in this analysis. Coordinates for the pericentromeres and centromeres in the reference genome are attributed to (Underwood et al., 2018). A Bonferroni threshold was used to determine significance for these tests.

GWA with enrichment for significant SNPs in the pericentromere and centromere were considered to be localized to a specific centromere if they had at least half of their significant SNPs present within the centromere.

The effect of an allele on sequence abundance was calculated by taking the harmonic mean of sequence abundance across individuals possessing the allele and comparing the value to the respective mean for individuals with the alternative allele.

Meta-analyses of genome-wide association of sequence abundance variation

Meta-GWAS analyses were performed separately for retrotransposons, DNA transposons, and simple repeats by combining p-values from genome-wide association likelihood ratio tests using Fisher's method per the following equation: $\chi^2 = -2 \sum_{i=1}^{k} log\,(pi)$ (Evangelou and Ioannidis, 2013) where *k* is the number of studies included in the meta-analysis and p_i is the p-value for a variant in study *i.* Individual studies with excess significant variants per Bonferroni threshold and studies in which the K-mer based sequence abundance estimates were strongly correlated (Spearman's ρ rho > 0.60) were excluded from analysis.

To correct for test statistic inflation across studies included in the meta-analyses, the genomic inflation factor, λ, was calculated and used to correct the chi-squared values. λ was calculated as follows: $\lambda = median\,(\chi^2\ observed)\ /\ median\,(\chi^2\ expected)$ where the median expected χ^2value is the value at the 0.5 / k quantile of observed values. Focal variants were considered to be the set of SNPs with the top 0.1% of χ^2value per meta-analysis.

Gene ontology enrichment analysis

Gene ontology enrichment analysis was done with topGO 2.46.0 (Alexa and Rahnenfuhrer, 2019) using the “weight01” algorithm and Fisher’s exact test. Genes of interest were considered to be genes within 10 KB of focal meta-GWA SNPs for all three meta-GWA analyses. Genes were considered to be significantly enriched if $p < 0.05$.

Evolutionary analyses

Allele frequencies were calculated using plink 1.9 (Chang et al., 2015). Alleles were assigned ancestral or derived state based on an alignment of the TAIR10 genome assembly to the *Arabidopsis lyrata* v.1 assembly (Hu et al., 2011) using minimap2 v. 2.17 (Li, 2018) using the “asm10” parameter. Only sites with segregating ancestral and derived alleles in *A. thaliana* were considered for further analysis. Variants were classified as nonsynonymous or synonymous based on annotating the 1001 Genomes VCF using the Araport11 annotation (Cheng et al., 2017) and Variant Effect Predictor v. 103.1 (McLaren et al., 2016). Associated variants from AraGWAS (Togninalli et al., 2020, 2018) were accessed on 2021-09-01 and consisted of 44,680 significant associations across 462 studies.

Sequences with copy number change were identified by testing whether the median sequence abundance per group was different from the median abundance in Africa, the presumed progenitor to all other groups, using Wilcoxon-Mann Whitney U test in R (R Core Team, 2013). Bonferroni-adjusted alpha of 0.05 was used to determine significance.

Acknowledgments

We thank Danelle K. Seymour, Keely E. Brown, Jacob B. Landis, Jason E. Stajich, and Zhenyu (Arthur) Jia for their helpful comments and suggestions that improved this work. All computational analyses were performed using resources at the High Performance Computing Center at the University of California, Riverside, supported by NSF grants MRI-2215705 and MRI-1429826, and NIH grant 1S10OD016290-01A1. D.K. is supported by NSF CAREER grant IOS-2046256.

Data Availability Statement

A user-friendly generalizable version of the K-mer pipeline is available at GitHub at https://github.com/cjfiscus/Kmer-it. The 12-mer based sequence abundance estimates along with an archived version of the K-mer pipeline that was used to generate the data for this manuscript are available from figshare at https://figshare.com/articles/dataset/Resources_for_Fiscus_CJ_Koenig_D_The_genetic_control_of_rapid_genome_content_divergence_in_Arabidopsis_thaliana_bioRxiv_2025_p_2025_06_11_659220_doi_10_1101_2025_06_11_659220_/29422016. All other data and methods required to reproduce this work are described within the manuscript or the supplementary material.

References

1001 Genomes Consortium. 2016. 1,135 Genomes Reveal the Global Pattern of Polymorphism in Arabidopsis thaliana. *Cell* **166**:481–491.

Adams MD, Celniker SE, Holt RA, Evans CA, Gocayne JD, Amanatides PG, Scherer SE, Li PW, Hoskins RA, Galle RF, George RA, Lewis SE, Richards S, Ashburner M, Henderson SN,

807 Sutton GG, Wortman JR, Yandell MD, Zhang Q, Chen LX, Brandon RC, Rogers YH, Blazej
808 RG, Champe M, Pfeiffer BD, Wan KH, Doyle C, Baxter EG, Helt G, Nelson CR, Gabor GL,
809 Abril JF, Agbayani A, An HJ, Andrews-Pfannkoch C, Baldwin D, Ballew RM, Basu A,
810 Baxendale J, Bayraktaroglu L, Beasley EM, Beeson KY, Benos PV, Berman BP, Bhandari D,
811 Bolshakov S, Borkova D, Botchan MR, Bouck J, Brokstein P, Brottier P, Burtis KC, Busam
812 DA, Butler H, Cadieu E, Center A, Chandra I, Cherry JM, Cawley S, Dahlke C, Davenport
813 LB, Davies P, de Pablos B, Delcher A, Deng Z, Mays AD, Dew I, Dietz SM, Dodson K, Doup
814 LE, Downes M, Dugan-Rocha S, Dunkov BC, Dunn P, Durbin KJ, Evangelista CC, Ferraz C,
815 Ferriera S, Fleischmann W, Fosler C, Gabrielian AE, Garg NS, Gelbart WM, Glasser K,
816 Glodek A, Gong F, Gorrell JH, Gu Z, Guan P, Harris M, Harris NL, Harvey D, Heiman TJ,
817 Hernandez JR, Houck J, Hostin D, Houston KA, Howland TJ, Wei MH, Ibegwam C, Jalali
818 M, Kalush F, Karpen GH, Ke Z, Kennison JA, Ketchum KA, Kimmel BE, Kodira CD, Kraft C,
819 Kravitz S, Kulp D, Lai Z, Lasko P, Lei Y, Levitsky AA, Li J, Li Z, Liang Y, Lin X, Liu X, Mattei
820 B, McIntosh TC, McLeod MP, McPherson D, Merkulov G, Milshina NV, Mobarry C, Morris
821 J, Moshrefi A, Mount SM, Moy M, Murphy B, Murphy L, Muzny DM, Nelson DL, Nelson
822 DR, Nelson KA, Nixon K, Nusskern DR, Pacleb JM, Palazzolo M, Pittman GS, Pan S,
823 Pollard J, Puri V, Reese MG, Reinert K, Remington K, Saunders RD, Scheeler F, Shen H,
824 Shue BC, Sidén-Kiamos I, Simpson M, Skupski MP, Smith T, Spier E, Spradling AC,
825 Stapleton M, Strong R, Sun E, Svirskas R, Tector C, Turner R, Venter E, Wang AH, Wang X,
826 Wang ZY, Wassarman DA, Weinstock GM, Weissenbach J, Williams SM, WoodageT,
827 Worley KC, Wu D, Yang S, Yao QA, Ye J, Yeh RF, Zaveri JS, Zhan M, Zhang G, Zhao Q,
828 Zheng L, Zheng XH, Zhong FN, Zhong W, Zhou X, Zhu S, Zhu X, Smith HO, Gibbs RA,
829 Myers EW, Rubin GM, Venter JC. 2000. The genome sequence of Drosophila
830 melanogaster. *Science* **287**:2185–2195.
831 Aird D, Ross MG, Chen W-S, Danielsson M, Fennell T, Russ C, Jaffe DB, Nusbaum C, Gnirke A.
832 2011. Analyzing and minimizing PCR amplification bias in Illumina sequencing libraries.
833 *Genome Biol* **12**:R18. doi:10.1186/gb-2011-12-2-r18
834 Alexa A, Rahnenfuhrer J. 2019. topGO: Enrichment Analysis for Gene Ontology.
835 Arabidopsis Genome Initiative. 2000. Analysis of the genome sequence of the flowering plant
836 Arabidopsis thaliana. *Nature* **408**:796–815.
837 Armstrong J, Hickey G, Diekhans M, Fiddes IT, Novak AM, Deran A, Fang Q, Xie D, Feng S,
838 Stiller J, Genereux D, Johnson J, Marinescu VD, Alföldi J, Harris RS, Lindblad-Toh K,
839 Haussler D, Karlsson E, Jarvis ED, Zhang G, Paten B. 2020. Progressive Cactus is a
840 multiple-genome aligner for the thousand-genome era. *Nature* **587**:246–251.
841 doi:10.1038/s41586-020-2871-y
842 Ayala-García VM, Baruch-Torres N, García-Medel PL, Brieba LG. 2018. Plant organellar DNA
843 polymerases paralogs exhibit dissimilar nucleotide incorporation fidelity. *FEBS J*
844 **285**:4005–4018. doi:10.1111/febs.14645
845 Baduel P, Leduque B, Ignace A, Gy I, Gil J, Loudet O, Colot V, Quadrana L. 2021. Genetic and
846 environmental modulation of transposition shapes the evolutionary potential of Arabidopsis
847 thaliana. *Genome Biol* **22**:1–26.
848 Bankevich A, Nurk S, Antipov D, Gurevich AA, Dvorkin M, Kulikov AS, Lesin VM, Nikolenko SI,
849 Pham S, Prjibelski AD, Pyshkin AV, Sirotkin AV, Vyahhi N, Tesler G, Alekseyev MA, Pevzner
850 PA. 2012. SPAdes: a new genome assembly algorithm and its applications to single-cell
851 sequencing. *J Comput Biol* **19**:455–477. doi:10.1089/cmb.2012.0021
852 Bao W, Kojima KK, Kohany O. 2015. Repbase Update, a database of repetitive elements in

eukaryotic genomes. *Mob DNA* **6**:11.
Bolger AM, Lohse M, Usadel B. 2014. Trimmomatic: a flexible trimmer for Illumina sequence data. *Bioinformatics* **30**:2114–2120. doi:10.1093/bioinformatics/btu170
Bosco G, Campbell P, Leiva-Neto JT, Markow TA. 2007. Analysis of Drosophila species genome size and satellite DNA content reveals significant differences among strains as well as between species. *Genetics* **177**:1277–1290.
Braz ASK, Finnegan J, Waterhouse P, Margis R. 2004. A plant orthologue of RNase L inhibitor (RLI) is induced in plants showing RNA interference. *J Mol Evol* **59**:20–30. doi:10.1007/s00239-004-2600-4
Britten RJ, Graham DE, Neufeld BR. 1974. [29] Analysis of repeating DNA sequences by reassociationMethods in Enzymology. Academic Press. pp. 363–418.
Britten RJ, Kohne DE. 1968. Repeated sequences in DNA. *Science* **161**:529–540.
Campi M, D'Andrea L, Emiliani J, Casati P. 2012. Participation of chromatin-remodeling proteins in the repair of ultraviolet-B-damaged DNA. *Plant Physiol* **158**:981–995. doi:10.1104/pp.111.191452
Chakravarti D, LaBella KA, DePinho RA. 2021. Telomeres: history, health, and hallmarks of aging. *Cell* **184**:306–322. doi:10.1016/j.cell.2020.12.028
Chang CC, Chow CC, Tellier LC, Vattikuti S, Purcell SM, Lee JJ. 2015. Second-generation PLINK: rising to the challenge of larger and richer datasets. *Gigascience* **4**:7. doi:10.1186/s13742-015-0047-8
Cheng C-Y, Krishnakumar V, Chan AP, Thibaud-Nissen F, Schobel S, Town CD. 2017. Araport11: a complete reannotation of the Arabidopsis thaliana reference genome. *Plant J* **89**:789–804.
Choi JY, Abdulkina LR, Yin J, Chastukhina IB, Lovell JT, Agabekian IA, Young PG, Razzaque S, Shippen DE, Juenger TE, Shakirov EV, Purugganan MD. 2021. Natural variation in plant telomere length is associated with flowering time. *Plant Cell* **33**:1118–1134.
Choi K, Reinhard C, Serra H, Ziolkowski PA, Underwood CJ, Zhao X, Hardcastle TJ, Yelina NE, Griffin C, Jackson M, Mézard C, McVean G, Copenhaver GP, Henderson IR. 2016. Recombination rate heterogeneity within Arabidopsis disease resistance genes. *PLoS Genet* **12**:e1006179. doi:10.1371/journal.pgen.1006179
Cochetel N, Minio A, Guarracino A, Garcia JF, Figueroa-Balderas R, Massonnet M, Londo J, Garrison E, Gaut B, Cantu D. 2023. A reference-unbiased super-pangenome of the North American wild grape species (Vitis spp.) reveals genus-wide association with adaptive traits. *bioRxiv*. doi:10.1101/2023.06.27.545624
Corradi N, Pombert J-F, Farinelli L, Didier ES, Keeling PJ. 2010. The complete sequence of the smallest known nuclear genome from the microsporidian Encephalitozoon intestinalis. *Nat Commun* **1**:77. doi:10.1038/ncomms1082
Davison J, Tyagi A, Comai L. 2007. Large-scale polymorphism of heterochromatic repeats in the DNA of Arabidopsis thaliana. *BMC Plant Biol* **7**:44.
de la Chaux N, Tsuchimatsu T, Shimizu KK, Wagner A. 2012. The predominantly selfing plant Arabidopsis thaliana experienced a recent reduction in transposable element abundance compared to its outcrossing relative Arabidopsis lyrata. *Mob DNA* **3**:2.
Doutriaux MP, Couteau F, Bergounioux C, White C. 1998. Isolation and characterisation of the RAD51 and DMC1 homologs from Arabidopsis thaliana. *Mol Gen Genet* **257**:283–291. doi:10.1007/s004380050649
Durvasula A, Fulgione A, Gutaker RM, Alacakaptan SI, Flood PJ, Neto C, Tsuchimatsu T,

Burbano HA, Picó FX, Alonso-Blanco C, Hancock AM. 2017. African genomes illuminate the early history and transition to selfing in Arabidopsis thaliana. *Proc Natl Acad Sci U S A* **114**:5213–5218.

Elliott TA, Gregory TR. 2015. What's in a genome? The C-value enigma and the evolution of eukaryotic genome content. *Philos Trans R Soc Lond B Biol Sci* **370**:20140331. doi:10.1098/rstb.2014.0331

Evangelou E, Ioannidis JPA. 2013. Meta-analysis methods for genome-wide association studies and beyond. *Nat Rev Genet* **14**:379–389. doi:10.1038/nrg3472

Fernandes JB, Naish M, Lian Q, Burns R, Tock AJ, Rabanal FA, Wlodzimierz P, Habring A, Nicholas RE, Weigel D, Mercier R, Henderson IR. 2024. Structural variation and DNA methylation shape the centromere-proximal meiotic crossover landscape in Arabidopsis. *Genome Biol* **25**:30. doi:10.1186/s13059-024-03163-4

Gadgil RY, Romer EJ, Goodman CC, Rider SD Jr, Damewood FJ, Barthelemy JR, Shin-Ya K, Hanenberg H, Leffak M. 2020. Replication stress at microsatellites causes DNA double-strand breaks and break-induced replication. *J Biol Chem* **295**:15378–15397. doi:10.1074/jbc.RA120.013495

Göktay M, Fulgione A, Hancock AM. 2020. A new catalog of structural variants in 1,301 A. thaliana lines from Africa, Eurasia, and North America reveals a signature of balancing selection at defense response genes. *Mol Biol Evol* **38**:1498–1511. doi:10.1093/molbev/msaa309

Golicz AA, Bayer PE, Barker GC, Edger PP, Kim H, Martinez PA, Chan CKK, Severn-Ellis A, McCombie WR, Parkin IAP, Paterson AH, Pires JC, Sharpe AG, Tang H, Teakle GR, Town CD, Batley J, Edwards D. 2016. The pangenome of an agronomically important crop plant Brassica oleracea. *Nat Commun* **7**:13390. doi:10.1038/ncomms13390

Gong Z, Morales-Ruiz T, Ariza RR, Roldán-Arjona T, David L, Zhu JK. 2002. ROS1, a repressor of transcriptional gene silencing in Arabidopsis, encodes a DNA glycosylase/lyase. *Cell* **111**:803–814. doi:10.1016/s0092-8674(02)01133-9

Gordon SP, Contreras-Moreira B, Woods DP, Des Marais DL, Burgess D, Shu S, Stritt C, Roulin AC, Schackwitz W, Tyler L, Martin J, Lipzen A, Dochy N, Phillips J, Barry K, Geuten K, Budak H, Juenger TE, Amasino R, Caicedo AL, Goodstein D, Davidson P, Mur LAJ, Figueroa M, Freeling M, Catalan P, Vogel JP. 2017. Extensive gene content variation in the Brachypodium distachyon pan-genome correlates with population structure. *Nat Commun* **8**:2184.

Gregory TR. 2001. Coincidence, coevolution, or causation? DNA content, cell size, and the C-value enigma. *Biol Rev Camb Philos Soc* **76**:65–101.

Hickman AB, Dyda F. 2015. Mechanisms of DNA transpositionMobile DNA III. American Society of Microbiology. pp. 531–553. doi:10.1128/microbiolspec.mdna3-0034-2014

Hohmann N, Wolf EM, Lysak MA, Koch MA. 2015. A Time-Calibrated Road Map of Brassicaceae Species Radiation and Evolutionary History. *Plant Cell* **27**:2770–2784.

Hollister JD, Gaut BS. 2009. Epigenetic silencing of transposable elements: a trade-off between reduced transposition and deleterious effects on neighboring gene expression. *Genome Res* **19**:1419–1428.

Huang W, Li L, Myers JR, Marth GT. 2012. ART: a next-generation sequencing read simulator. *Bioinformatics* **28**:593–594. doi:10.1093/bioinformatics/btr708

Hu TT, Pattyn P, Bakker EG, Cao J, Cheng J-F, Clark RM, Fahlgren N, Fawcett JA, Grimwood J, Gundlach H, Haberer G, Hollister JD, Ossowski S, Ottilar RP, Salamov AA, Schneeberger

K, Spannagl M, Wang X, Yang L, Nasrallah ME, Bergelson J, Carrington JC, Gaut BS, Schmutz J, Mayer KFX, Van de Peer Y, Grigoriev IV, Nordborg M, Weigel D, Guo Y-L. 2011. The Arabidopsis lyrata genome sequence and the basis of rapid genome size change. *Nat Genet* **43**:476–481.

Kang M, Wu H, Liu H, Liu W, Zhu M, Han Y, Liu W, Chen C, Song Y, Tan L, Yin K, Zhao Y, Yan Z, Lou S, Zan Y, Liu J. 2023. The pan-genome and local adaptation of Arabidopsis thaliana. *Nat Commun* **14**:6259. doi:10.1038/s41467-023-42029-4

Kim Y-K, Kim S, Shin Y-J, Hur Y-S, Kim W-Y, Lee M-S, Cheon C-I, Verma DPS. 2014. Ribosomal protein S6, a target of rapamycin, is involved in the regulation of rRNA genes by possible epigenetic changes in Arabidopsis. *J Biol Chem* **289**:3901–3912. doi:10.1074/jbc.M113.515015

Kriventseva EV, Kuznetsov D, Tegenfeldt F, Manni M, Dias R, Simão FA, Zdobnov EM. 2019. OrthoDB v10: sampling the diversity of animal, plant, fungal, protist, bacterial and viral genomes for evolutionary and functional annotations of orthologs. *Nucleic Acids Res* **47**:D807–D811. doi:10.1093/nar/gky1053

Kurzbauer M-T, Pradillo M, Kerzendorfer C, Sims J, Ladurner R, Oliver C, Janisiw MP, Mosiolek M, Schweizer D, Copenhaver GP, Schlögelhofer P. 2018. Arabidopsis thaliana FANCD2 Promotes Meiotic Crossover Formation. *Plant Cell* **30**:415–428. doi:10.1105/tpc.17.00745

Lamesch P, Berardini TZ, Li D, Swarbreck D, Wilks C, Sasidharan R, Muller R, Dreher K, Alexander DL, Garcia-Hernandez M, Karthikeyan AS, Lee CH, Nelson WD, Ploetz L, Singh S, Wensel A, Huala E. 2012. The Arabidopsis Information Resource (TAIR): improved gene annotation and new tools. *Nucleic Acids Res* **40**:D1202–10.

Lander ES, Linton LM, Birren B, Nusbaum C, Zody MC, Baldwin J, Devon K, Dewar K, Doyle M, FitzHugh W, Funke R, Gage D, Harris K, Heaford A, Howland J, Kann L, Lehoczky J, LeVine R, McEwan P, McKernan K, Meldrim J, Mesirov JP, Miranda C, Morris W, Naylor J, Raymond C, Rosetti M, Santos R, Sheridan A, Sougnez C, Stange-Thomann Y, Stojanovic N, Subramanian A, Wyman D, Rogers J, Sulston J, Ainscough R, Beck S, Bentley D, Burton J, Clee C, Carter N, Coulson A, Deadman R, Deloukas P, Dunham A, Dunham I, Durbin R, French L, Grafham D, Gregory S, Hubbard T, Humphray S, Hunt A, Jones M, Lloyd C, McMurray A, Matthews L, Mercer S, Milne S, Mullikin JC, Mungall A, Plumb R, Ross M, Shownkeen R, Sims S, Waterston RH, Wilson RK, Hillier LW, McPherson JD, Marra MA, Mardis ER, Fulton LA, Chinwalla AT, Pepin KH, Gish WR, Chissoe SL, Wendl MC, Delehaunty KD, Miner TL, Delehaunty A, Kramer JB, Cook LL, Fulton RS, Johnson DL, Minx PJ, Clifton SW, Hawkins T, Branscomb E, Predki P, Richardson P, Wenning S, Slezak T, Doggett N, Cheng JF, Olsen A, Lucas S, Elkin C, Uberbacher E, Frazier M, Gibbs RA, Muzny DM, Scherer SE, Bouck JB, Sodergren EJ, Worley KC, Rives CM, Gorrell JH, Metzker ML, Naylor SL, Kucherlapati RS, Nelson DL, Weinstock GM, Sakaki Y, Fujiyama A, Hattori M, Yada T, Toyoda A, Itoh T, Kawagoe C, Watanabe H, Totoki Y, Taylor T, Weissenbach J, Heilig R, Saurin W, Artiguenave F, Brottier P, Bruls T, Pelletier E, Robert C, Wincker P, Smith DR, Doucette-Stamm L, Rubenfield M, Weinstock K, Lee HM, Dubois J, Rosenthal A, Platzer M, Nyakatura G, Taudien S, Rump A, Yang H, Yu J, Wang J, Huang G, Gu J, Hood L, Rowen L, Madan A, Qin S, Davis RW, Federspiel NA, Abola AP, Proctor MJ, Myers RM, Schmutz J, Dickson M, Grimwood J, Cox DR, Olson MV, Kaul R, Raymond C, Shimizu N, Kawasaki K, Minoshima S, Evans GA, Athanasiou M, Schultz R, Roe BA, Chen F, Pan H, Ramser J, Lehrach H, Reinhardt R, McCombie WR, de la Bastide M, Dedhia N, Blöcker H, Hornischer K, Nordsiek G, Agarwala R, Aravind L, Bailey JA, Bateman A,

Batzoglou S, Birney E, Bork P, Brown DG, Burge CB, Cerutti L, Chen HC, Church D, Clamp M, Copley RR, Doerks T, Eddy SR, Eichler EE, Furey TS, Galagan J, Gilbert JG, Harmon C, Hayashizaki Y, Haussler D, Hermjakob H, Hokamp K, Jang W, Johnson LS, Jones TA, Kasif S, Kaspryzk A, Kennedy S, Kent WJ, Kitts P, Koonin EV, Korf I, Kulp D, Lancet D, Lowe TM, McLysaght A, Mikkelsen T, Moran JV, Mulder N, Pollara VJ, Ponting CP, Schuler G, Schultz J, Slater G, Smit AF, Stupka E, Szustakowki J, Thierry-Mieg D, Thierry-Mieg J, Wagner L, Wallis J, Wheeler R, Williams A, Wolf YI, Wolfe KH, Yang SP, Yeh RF, Collins F, Guyer MS, Peterson J, Felsenfeld A, Wetterstrand KA, Patrinos A, Morgan MJ, de Jong P, Catanese JJ, Osoegawa K, Shizuya H, Choi S, Chen YJ, Szustakowki J, International Human Genome Sequencing Consortium. 2001. Initial sequencing and analysis of the human genome. *Nature* **409**:860–921.

Le TN, Miyazaki Y, Takuno S, Saze H. 2015. Epigenetic regulation of intragenic transposable elements impacts gene transcription in Arabidopsis thaliana. *Nucleic Acids Res* **43**:3911–3921.

Lian Q, Huettel B, Walkemeier B, Mayjonade B, Lopez-Roques C, Gil L, Roux F, Schneeberger K, Mercier R. 2024. A pan-genome of 69 Arabidopsis thaliana accessions reveals a conserved genome structure throughout the global species range. *Nat Genet*. doi:10.1038/s41588-024-01715-9

Li H. 2018. Minimap2: pairwise alignment for nucleotide sequences. *Bioinformatics* **34**:3094–3100. doi:10.1093/bioinformatics/bty191

Li H. 2013. Aligning sequence reads, clone sequences and assembly contigs with BWA-MEM. *arXiv [q-bioGN]*.

Li H. n.d. seqtk: Toolkit for processing sequences in FASTA/Q formats. *Github*. https://github.com/lh3/seqtk

Li H, Durbin R. 2009. Fast and accurate short read alignment with Burrows-Wheeler transform. *Bioinformatics* **25**:1754–1760. doi:10.1093/bioinformatics/btp324

Li H, Handsaker B, Wysoker A, Fennell T, Ruan J, Homer N, Marth G, Abecasis G, Durbin R, 1000 Genome Project Data Processing Subgroup. 2009. The Sequence Alignment/Map format and SAMtools. *Bioinformatics* **25**:2078–2079. doi:10.1093/bioinformatics/btp352

Lindroth AM, Cao X, Jackson JP, Zilberman D, McCallum CM, Henikoff S, Jacobsen SE. 2001. Requirement of CHROMOMETHYLASE3 for maintenance of CpXpG methylation. *Science* **292**:2077–2080. doi:10.1126/science.1059745

Liu S, Zheng J, Migeon P, Ren J, Hu Y, He C, Liu H, Fu J, White FF, Toomajian C, Wang G. 2017. Unbiased K-mer Analysis Reveals Changes in Copy Number of Highly Repetitive Sequences During Maize Domestication and Improvement. *Sci Rep* **7**:42444.

Liu Y, Du H, Li P, Shen Y, Peng H, Liu S, Zhou G-A, Zhang H, Liu Z, Shi M, Huang X, Li Y, Zhang M, Wang Z, Zhu B, Han B, Liang C, Tian Z. 2020. Pan-genome of wild and cultivated soybeans. *Cell* **182**:162–176.e13. doi:10.1016/j.cell.2020.05.023

Li W, Chen C, Markmann-Mulisch U, Timofejeva L, Schmelzer E, Ma H, Reiss B. 2004. The *Arabidopsis AtRAD51* gene is dispensable for vegetative development but required for meiosis. *Proc Natl Acad Sci U S A* **101**:10596–10601. doi:10.1073/pnas.0404110101

Long Q, Rabanal FA, Meng D, Huber CD, Farlow A, Platzer A, Zhang Q, Vilhjálmsson BJ, Korte A, Nizhynska V, Voronin V, Korte P, Sedman L, Mandáková T, Lysak MA, Seren Ü, Hellmann I, Nordborg M. 2013. Massive genomic variation and strong selection in Arabidopsis thaliana lines from Sweden. *Nat Genet* **45**:884–890.

Lu Y, Dai J, Yang L, La Y, Zhou S, Qiang S, Wang Q, Tan F, Wu Y, Kong W, La H. 2020.

Involvement of MEM1 in DNA demethylation in Arabidopsis. *Plant Mol Biol* **102**:307–322. doi:10.1007/s11103-019-00949-0

Maheshwari S, Ishii T, Brown CT, Houben A, Comai L. 2017. Centromere location in Arabidopsis is unaltered by extreme divergence in CENH3 protein sequence. *Genome Res* **27**:471–478.

Marçais G, Kingsford C. 2011. A fast, lock-free approach for efficient parallel counting of occurrences of k-mers. *Bioinformatics* **27**:764–770. doi:10.1093/bioinformatics/btr011

Masuda HP, Ramos GBA, de Almeida-Engler J, Cabral LM, Coqueiro VM, Macrini CMT, Ferreira PCG, Hemerly AS. 2004. Genome based identification and analysis of the pre-replicative complex of Arabidopsis thaliana. *FEBS Lett* **574**:192–202. doi:10.1016/j.febslet.2004.07.088

McLaren W, Gil L, Hunt SE, Riat HS, Ritchie GRS, Thormann A, Flicek P, Cunningham F. 2016. The Ensembl Variant Effect Predictor. *Genome Biol* **17**:122. doi:10.1186/s13059-016-0974-4

Mehrotra S, Goyal V. 2014. Repetitive sequences in plant nuclear DNA: types, distribution, evolution and function. *Genomics Proteomics Bioinformatics* **12**:164–171.

Montenegro JD, Golicz AA, Bayer PE, Hurgobin B, Lee H, Chan C-KK, Visendi P, Lai K, Doležel J, Batley J, Edwards D. 2017. The pangenome of hexaploid bread wheat. *Plant J* **90**:1007–1013. doi:10.1111/tpj.13515

Nikolenko SI, Korobeynikov AI, Alekseyev MA. 2013. BayesHammer: Bayesian clustering for error correction in single-cell sequencing. *BMC Genomics* **14 Suppl 1**:S7. doi:10.1186/1471-2164-14-S1-S7

Novák P, Guignard MS, Neumann P, Kelly LJ, Mlinarec J, Koblížková A, Dodsworth S, Kovařík A, Pellicer J, Wang W, Macas J, Leitch IJ, Leitch AR. 2020. Repeat-sequence turnover shifts fundamentally in species with large genomes. *Nature Plants* **6**:1325–1329. doi:10.1038/s41477-020-00785-x

Novikova PY, Hohmann N, Nizhynska V, Tsuchimatsu T, Ali J, Muir G, Guggisberg A, Paape T, Schmid K, Fedorenko OM, Holm S, Säll T, Schlötterer C, Marhold K, Widmer A, Sese J, Shimizu KK, Weigel D, Krämer U, Koch MA, Nordborg M. 2016. Sequencing of the genus Arabidopsis identifies a complex history of nonbifurcating speciation and abundant trans-specific polymorphism. *Nat Genet* **48**:1077–1082.

Nurk S, Koren S, Rhie A, Rautiainen M, Bzikadze AV, Mikheenko A, Vollger MR, Altemose N, Uralsky L, Gershman A, Aganezov S, Hoyt SJ, Diekhans M, Logsdon GA, Alonge M, Antonarakis SE, Borchers M, Bouffard GG, Brooks SY, Caldas GV, Chen N-C, Cheng H, Chin C-S, Chow W, de Lima LG, Dishuck PC, Durbin R, Dvorkina T, Fiddes IT, Formenti G, Fulton RS, Fungtammasan A, Garrison E, Grady PGS, Graves-Lindsay TA, Hall IM, Hansen NF, Hartley GA, Haukness M, Howe K, Hunkapiller MW, Jain C, Jain M, Jarvis ED, Kerpedjiev P, Kirsche M, Kolmogorov M, Korlach J, Kremitzki M, Li H, Maduro VV, Marschall T, McCartney AM, McDaniel J, Miller DE, Mullikin JC, Myers EW, Olson ND, Paten B, Peluso P, Pevzner PA, Porubsky D, Potapova T, Rogaev EI, Rosenfeld JA, Salzberg SL, Schneider VA, Sedlazeck FJ, Shafin K, Shew CJ, Shumate A, Sims Y, Smit AFA, Soto DC, Sović I, Storer JM, Streets A, Sullivan BA, Thibaud-Nissen F, Torrance J, Wagner J, Walenz BP, Wenger A, Wood JMD, Xiao C, Yan SM, Young AC, Zarate S, Surti U, McCoy RC, Dennis MY, Alexandrov IA, Gerton JL, O'Neill RJ, Timp W, Zook JM, Schatz MC, Eichler EE, Miga KH, Phillippy AM. 2022. The complete sequence of a human genome. *Science* **376**:44–53.

Ohno S. 1972. So much ``junk'' DNA in our genome. *Brookhaven Symp Biol* **23**:366–370.
Ohtsubo T, Matsuda O, Iba K, Terashima I, Sekiguchi M, Nakabeppu Y. 1998. Molecular cloning of AtMMH, an Arabidopsis thaliana ortholog of the Escherichia coli mutM gene, and analysis of functional domains of its product. *Mol Gen Genet* **259**:577–590. doi:10.1007/s004380050851
Ou S, Su W, Liao Y, Chougule K, Agda JRA, Hellinga AJ, Lugo CSB, Elliott TA, Ware D, Peterson T, Jiang N, Hirsch CN, Hufford MB. 2019. Benchmarking transposable element annotation methods for creation of a streamlined, comprehensive pipeline. *Genome Biol* **20**:275.
Quadrana L, Bortolini Silveira A, Mayhew GF, LeBlanc C, Martienssen RA, Jeddeloh JA, Colot V. 2016. The Arabidopsis thaliana mobilome and its impact at the species level. *Elife* **5**.
Quesneville H. 2020. Twenty years of transposable element analysis in the Arabidopsis thaliana genome. *Mob DNA* **11**:28.
Quinlan AR, Hall IM. 2010. BEDTools: a flexible suite of utilities for comparing genomic features. *Bioinformatics* **26**:841–842. doi:10.1093/bioinformatics/btq033
Rabanal FA, Nizhynska V, Mandáková T, Novikova PY, Lysak MA, Mott R, Nordborg M. 2017. Unstable Inheritance of 45S rRNA Genes in Arabidopsis thaliana. *G3* **7**:1201–1209. doi:10.1534/g3.117.040204
R Core Team. 2023. R: A Language and Environment for Statistical Computing. Vienna, Austria: R Foundation for Statistical Computing.
R Core Team. 2013. R: A Language and Environment for Statistical Computing.
Ream TS, Haag JR, Wierzbicki AT, Nicora CD, Norbeck AD, Zhu J-K, Hagen G, Guilfoyle TJ, Pasa-Tolić L, Pikaard CS. 2009. Subunit compositions of the RNA-silencing enzymes Pol IV and Pol V reveal their origins as specialized forms of RNA polymerase II. *Mol Cell* **33**:192–203. doi:10.1016/j.molcel.2008.12.015
Ritchie ME, Phipson B, Wu D, Hu Y, Law CW, Shi W, Smyth GK. 2015. limma powers differential expression analyses for RNA-sequencing and microarray studies. *Nucleic Acids Res* **43**:e47. doi:10.1093/nar/gkv007
Rognes T, Flouri T, Nichols B, Quince C, Mahé F. 2016. VSEARCH: a versatile open source tool for metagenomics. *PeerJ* **4**:e2584. doi:10.7717/peerj.2584
Schiml S, Fauser F, Puchta H. 2016. Repair of adjacent single-strand breaks is often accompanied by the formation of tandem sequence duplications in plant genomes. *Proc Natl Acad Sci U S A* **113**:7266–7271. doi:10.1073/pnas.1603823113
Seeliger K, Dukowic-Schulze S, Wurz-Wildersinn R, Pacher M, Puchta H. 2012. BRCA2 is a mediator of RAD51- and DMC1-facilitated homologous recombination in Arabidopsis thaliana. *New Phytol* **193**:364–375. doi:10.1111/j.1469-8137.2011.03947.x
Serrano D, Cordero G, Kawamura R, Sverzhinsky A, Sarker M, Roy S, Malo C, Pascal JM, Marko JF, D'Amours D. 2020. The Smc5/6 Core Complex Is a Structure-Specific DNA Binding and Compacting Machine. *Mol Cell* **80**:1025–1038.e5. doi:10.1016/j.molcel.2020.11.011
Sievers A, Bosiek K, Bisch M, Dreessen C, Riedel J, Froß P, Hausmann M, Hildenbrand G. 2017. K-mer content, correlation, and position analysis of genome DNA sequences for the identification of function and evolutionary features. *Genes (Basel)* **8**:122. doi:10.3390/genes8040122
Simão FA, Waterhouse RM, Ioannidis P, Kriventseva EV, Zdobnov EM. 2015. BUSCO: assessing genome assembly and annotation completeness with single-copy orthologs.

Bioinformatics **31**:3210–3212. doi:10.1093/bioinformatics/btv351
Slotkin RK, Martienssen R. 2007. Transposable elements and the epigenetic regulation of the genome. *Nat Rev Genet* **8**:272–285.
Smit, AFA, Hubley, R & Green, P. 2013-2015. RepeatMasker Open-4.0.
Song B, Marco-Sola S, Moreto M, Johnson L, Buckler ES, Stitzer MC. 2022. AnchorWave: Sensitive alignment of genomes with high sequence diversity, extensive structural polymorphism, and whole-genome duplication. *Proc Natl Acad Sci U S A* **119**. doi:10.1073/pnas.2113075119
Springer PS, Holding DR, Groover A, Yordan C, Martienssen RA. 2000. The essential Mcm7 protein PROLIFERA is localized to the nucleus of dividing cells during the G(1) phase and is required maternally for early Arabidopsis development. *Development* **127**:1815–1822. doi:10.1242/dev.127.9.1815
Stanke M, Diekhans M, Baertsch R, Haussler D. 2008. Using native and syntenically mapped cDNA alignments to improve de novo gene finding. *Bioinformatics* **24**:637–644. doi:10.1093/bioinformatics/btn013
Stephan W. 1989. Tandem-repetitive noncoding DNA: forms and forces. *Mol Biol Evol* **6**:198–212.
Storer J, Hubley R, Rosen J, Wheeler TJ, Smit AF. 2021. The Dfam community resource of transposable element families, sequence models, and genome annotations. *Mob DNA* **12**:2. doi:10.1186/s13100-020-00230-y
Strzalka W, Ziemienowicz A. 2011. Proliferating cell nuclear antigen (PCNA): a key factor in DNA replication and cell cycle regulation. *Ann Bot* **107**:1127–1140. doi:10.1093/aob/mcq243
Sun H, Ding J, Piednoël M, Schneeberger K. 2018. findGSE: estimating genome size variation within human and Arabidopsis using k-mer frequencies. *Bioinformatics* **34**:550–557.
Talbert PB, Henikoff S. 2022. The genetics and epigenetics of satellite centromeres. *Genome Res* **32**:608–615. doi:10.1101/gr.275351.121
Togninalli M, Seren Ü, Freudenthal JA, Monroe JG, Meng D, Nordborg M, Weigel D, Borgwardt K, Korte A, Grimm DG. 2020. AraPheno and the AraGWAS Catalog 2020: a major database update including RNA-Seq and knockout mutation data for Arabidopsis thaliana. *Nucleic Acids Res* **48**:D1063–D1068.
Togninalli M, Seren Ü, Meng D, Fitz J, Nordborg M, Weigel D, Borgwardt K, Korte A, Grimm DG. 2018. The AraGWAS Catalog: a curated and standardized Arabidopsis thaliana GWAS catalog. *Nucleic Acids Res* **46**:D1150–D1156.
Treangen TJ, Salzberg SL. 2011. Repetitive DNA and next-generation sequencing: computational challenges and solutions. *Nat Rev Genet* **13**:36–46.
Turlan C, Chandler M. 2000. Playing second fiddle: second-strand processing and liberation of transposable elements from donor DNA. *Trends Microbiol* **8**:268–274. doi:10.1016/s0966-842x(00)01757-1
Underwood CJ, Choi K, Lambing C, Zhao X, Serra H, Borges F, Simorowski J, Ernst E, Jacob Y, Henderson IR, Martienssen RA. 2018. Epigenetic activation of meiotic recombination near Arabidopsis thaliana centromeres via loss of H3K9me2 and non-CG DNA methylation. *Genome Res* **28**:519–531. doi:10.1101/gr.227116.117
Verma P, Kumari P, Negi S, Yadav G, Gaur V. 2022. Holliday junction resolution by At-HIGLE: an SLX1 lineage endonuclease from Arabidopsis thaliana with a novel in-built regulatory mechanism. *Nucleic Acids Res* **50**:4630–4646. doi:10.1093/nar/gkac239

Voichek Y, Weigel D. 2020. Identifying genetic variants underlying phenotypic variation in plants without complete genomes. *Nat Genet* **52**:534–540. doi:10.1038/s41588-020-0612-7

Waterhouse RM, Seppey M, Simão FA, Manni M, Ioannidis P, Klioutchnikov G, Kriventseva EV, Zdobnov EM. 2018. BUSCO Applications from Quality Assessments to Gene Prediction and Phylogenomics. *Mol Biol Evol* **35**:543–548. doi:10.1093/molbev/msx319

Wei KH-C, Grenier JK, Barbash DA, Clark AG. 2014. Correlated variation and population differentiation in satellite DNA abundance among lines of Drosophila melanogaster. *Proc Natl Acad Sci U S A* **111**:18793–18798.

West CE, Waterworth WM, Jiang Q, Bray CM. 2000. Arabidopsis DNA ligase IV is induced by gamma-irradiation and interacts with an Arabidopsis homologue of the double strand break repair protein XRCC4. *Plant J* **24**:67–78. doi:10.1046/j.1365-313x.2000.00856.x

Wlodzimierz P, Rabanal FA, Burns R, Naish M, Primetis E, Scott A, Mandáková T, Gorringe N, Tock AJ, Holland D, Fritschi K, Habring A, Lanz C, Patel C, Schlegel T, Collenberg M, Mielke M, Nordborg M, Roux F, Shirsekar G, Alonso-Blanco C, Lysak MA, Novikova PY, Bousios A, Weigel D, Henderson IR. 2023. Cycles of satellite and transposon evolution in Arabidopsis centromeres. *Nature* **618**:557–565. doi:10.1038/s41586-023-06062-z

Wolter F, Schindele P, Beying N, Scheben A, Puchta H. 2021. Different DNA repair pathways are involved in single-strand break-induced genomic changes in plants. *Plant Cell* **33**:3454–3469. doi:10.1093/plcell/koab204

Yue J-X, Liti G. 2019. simuG: a general-purpose genome simulator. *Bioinformatics* **35**:4442–4444. doi:10.1093/bioinformatics/btz424

Zhao Q, Feng Q, Lu H, Li Y, Wang A, Tian Q, Zhan Q, Lu Y, Zhang L, Huang T, Wang Y, Fan D, Zhao Y, Wang Z, Zhou C, Chen J, Zhu C, Li W, Weng Q, Xu Q, Wang Z-X, Wei X, Han B, Huang X. 2018. Pan-genome analysis highlights the extent of genomic variation in cultivated and wild rice. *Nat Genet* **50**:278–284.

Zhou H, Su X, Song B. 2024. ACMGA: a reference-free multiple-genome alignment pipeline for plant species. *BMC Genomics* **25**:515. doi:10.1186/s12864-024-10430-y

Zhou J-X, Du P, Liu Z-W, Feng C, Cai X-W, He X-J. 2021. FVE promotes RNA-directed DNA methylation by facilitating the association of RNA polymerase V with chromatin. *Plant J* **107**:467–479. doi:10.1111/tpj.15302

Zhou X, Stephens M. 2012. Genome-wide efficient mixed-model analysis for association studies. *Nat Genet* **44**:821–824. doi:10.1038/ng.2310

Zmienko A, Marszalek-Zenczak M, Wojciechowski P, Samelak-Czajka A, Luczak M, Kozlowski P, Karlowski WM, Figlerowicz M. 2020. AthCNV: A Map of DNA Copy Number Variations in the Arabidopsis thaliana Genome. *Plant Cell*.

Zou Y-P, Hou X-H, Wu Q, Chen J-F, Li Z-W, Han T-S, Niu X-M, Yang L, Xu Y-C, Zhang J, Zhang F-M, Tan D, Tian Z, Gu H, Guo Y-L. 2017. Adaptation of Arabidopsis thaliana to the Yangtze River basin. *Genome Biol* **18**:239.

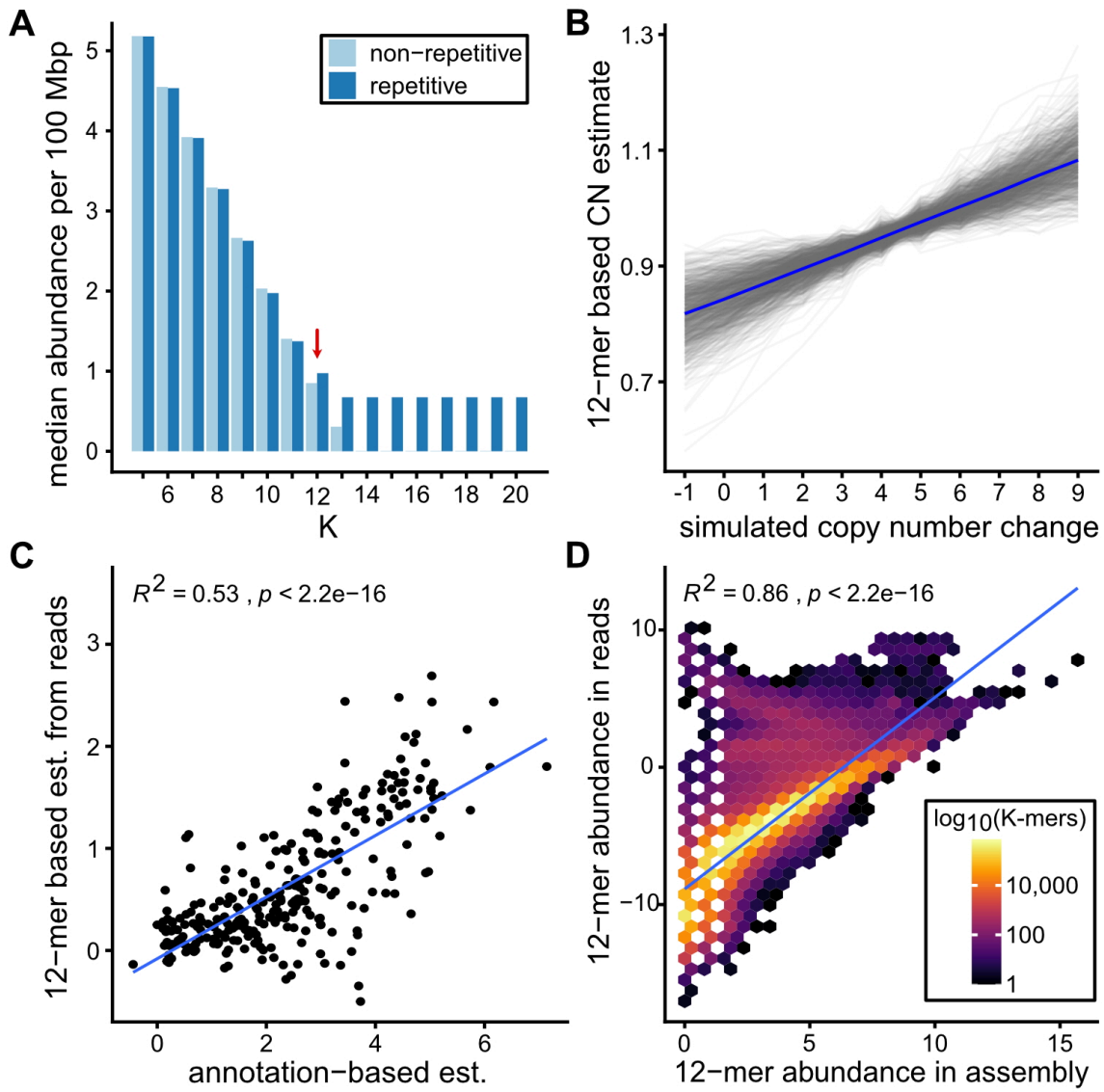

Figure 1. K-mer analyses of the *A. thaliana* reference genome
(A) Median K-mer frequency in the non-repetitive and repetitive compartments of the reference genome. (B) Relationship between scaled 12-mer based copy number estimates (y-axis) and simulated copy number change across 1,000 simulations. Each gray line denotes a single simulation iteration while the blue line indicates the median values across all iterations. (C) Relationship between 12-mer-based copy number estimates and annotation-based copy number estimates for 272 transposon families in the TAIR10 reference genome. Blue line indicates the line of best fit derived from the linear regression model. (D) Relationship between 12-mer abundances in Illumina reads (at 44 X mean coverage) compared to respective abundances in genome assembly. Each hexagonal bin is colored by the number of observations within the bin. Blue line indicates the line of best fit derived from the linear regression model.

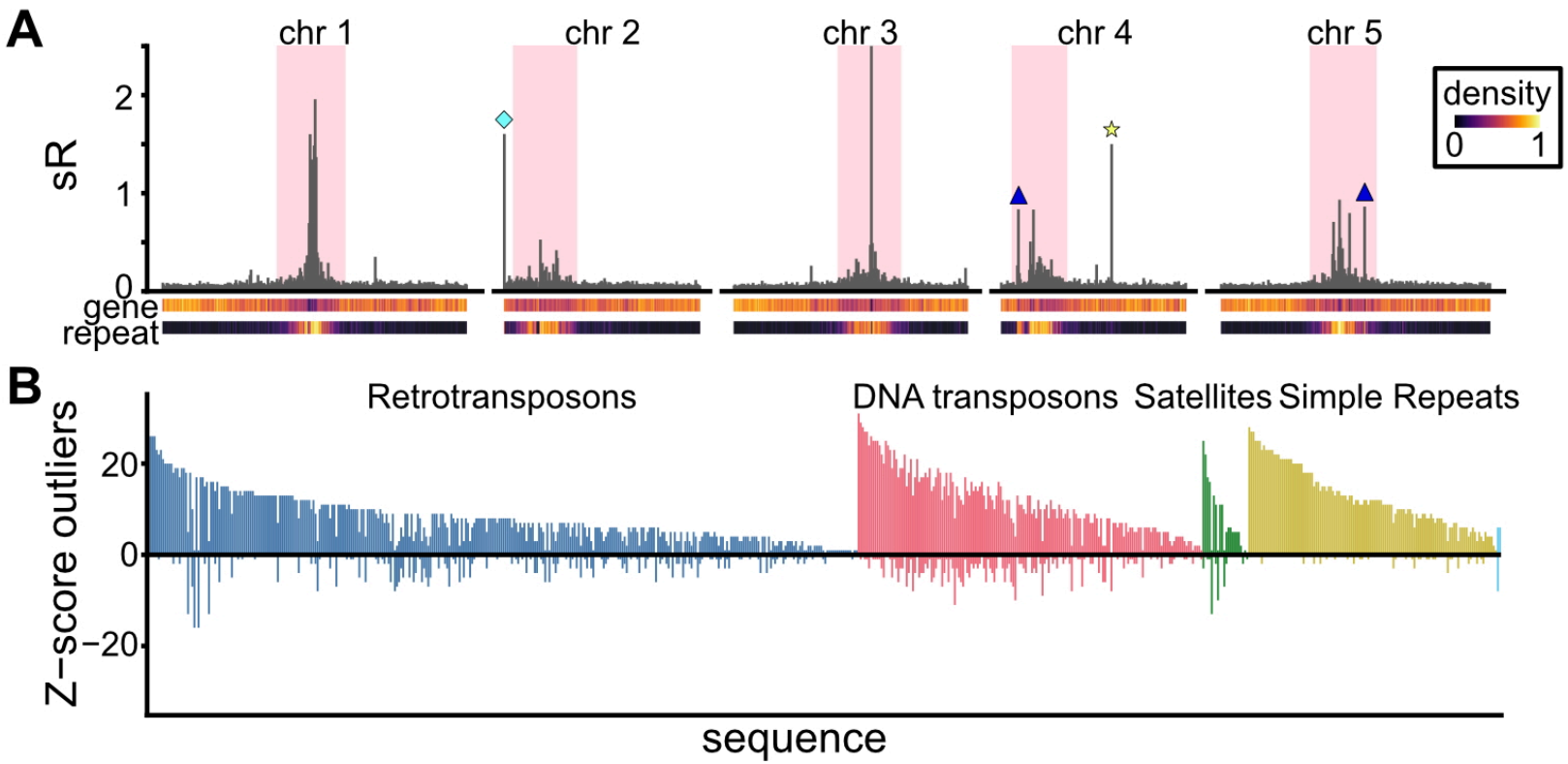

Figure 2. Patterns of copy number variability across the genome

(A) Sequence abundance variability in non-overlapping 100 KB windows across the genome compared to the density of genes and repeats. sR denotes the standardized range (range / median) of 12-mer abundance across all individuals. Pink shaded regions indicate the centromere and pericentromeric regions. Diamond = NOR2, triangles = knobs, star = cluster of cysteine-rich repeat proteins. (B) Number of individuals with putative copy number changes per repetitive sequence. Z-scores were calculated from the 12-mer derived copy number estimates and values on the Y axis correspond to the count of Z score values greater than (increase in copy number, positive value) or less than 3 (decrease in copy number, negative value) across sequences. Sequences colored teal are unclassified repeats.

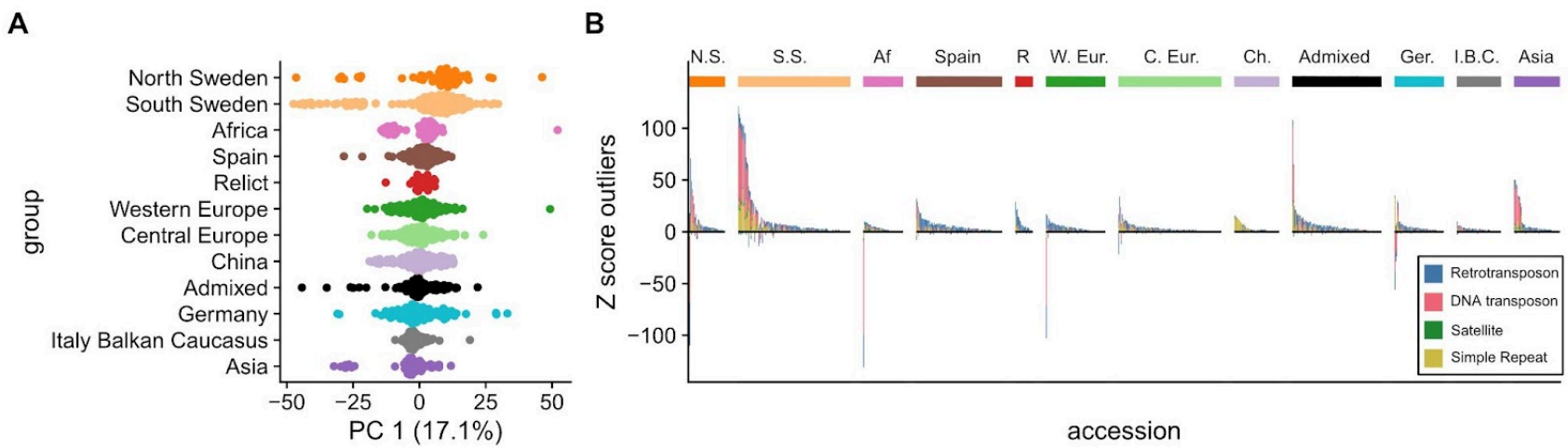

Figure 3. Repeat copy number differences between populations

(A) Principal component 1 of repeat copy number estimates partitioned by subpopulation. (B) Number of sequences with putative copy number change per individual grouped by subpopulation. Z-scores were calculated from the 12-mer derived copy number estimates and values on the Y axis correspond to the count of Z score values greater than (increase in copy number, positive value) or less than 3 (decrease in copy number, negative value) across individuals. Abbreviated subpopulations are as follows: N.S. is North Sweden, S.S. is South Sweden, Af. is Africa, R. is relict, W. Eur. is Western Europe, C. Eur. is Central Europe, Ch. is China, Ger. is Germany, I.B.C. is Italy Balkan Caucasus.

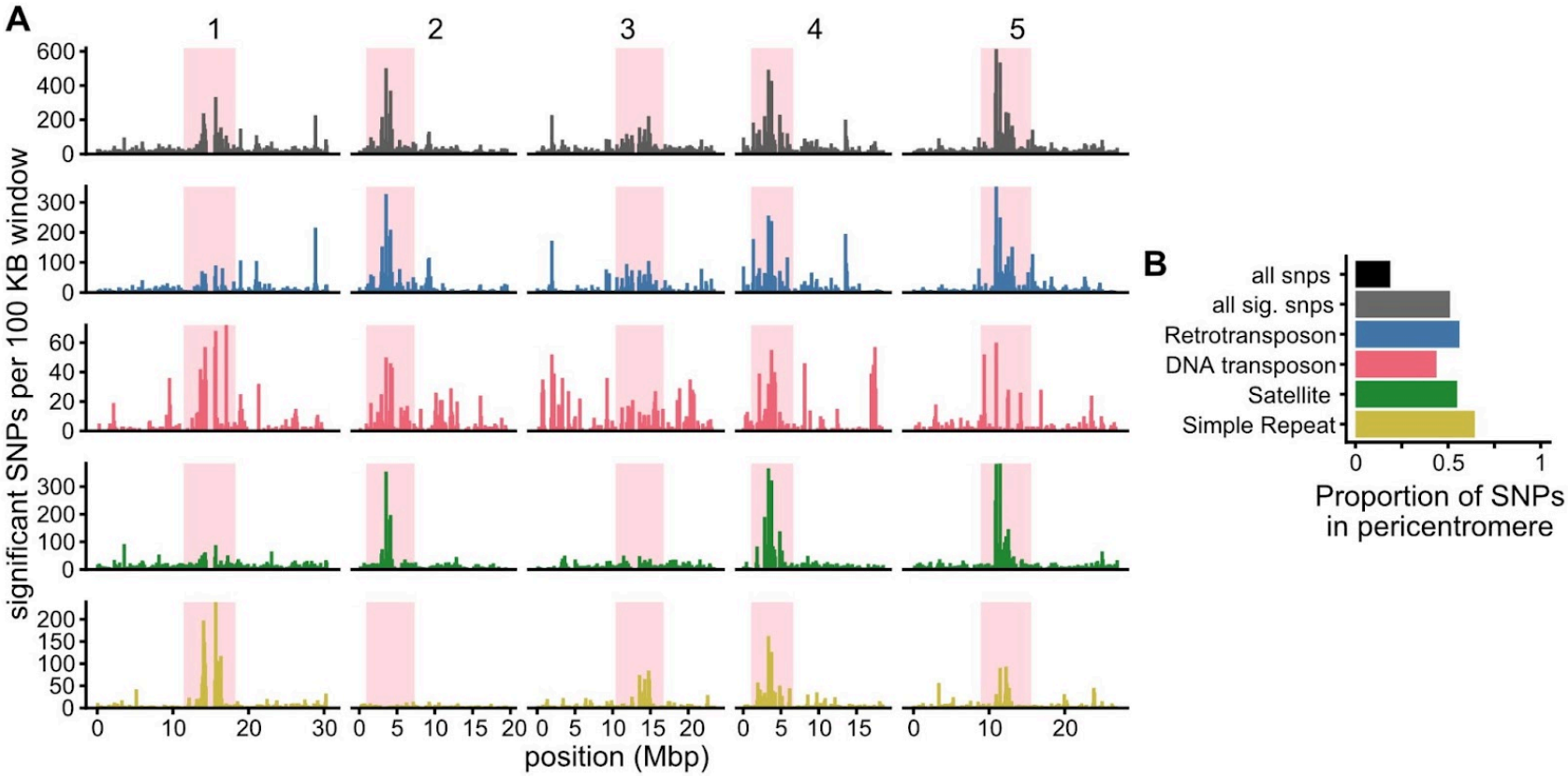

Figure 4. Genomic regions associated with repeat copy number variation.
(A) Frequency of significant SNPs per 100 KB windows for all GWAS (grey), or GWAS in retrotransposons (blue), DNA transposons (red), satellites (green), and simple repeats (yellow), respectively. Pink highlighted region indicates centromere and pericentromere. (B) Proportion of all SNPs (black), significant SNPs in all GWAS (grey), and significant SNPs in GWAS by sequence class in the pericentromere.

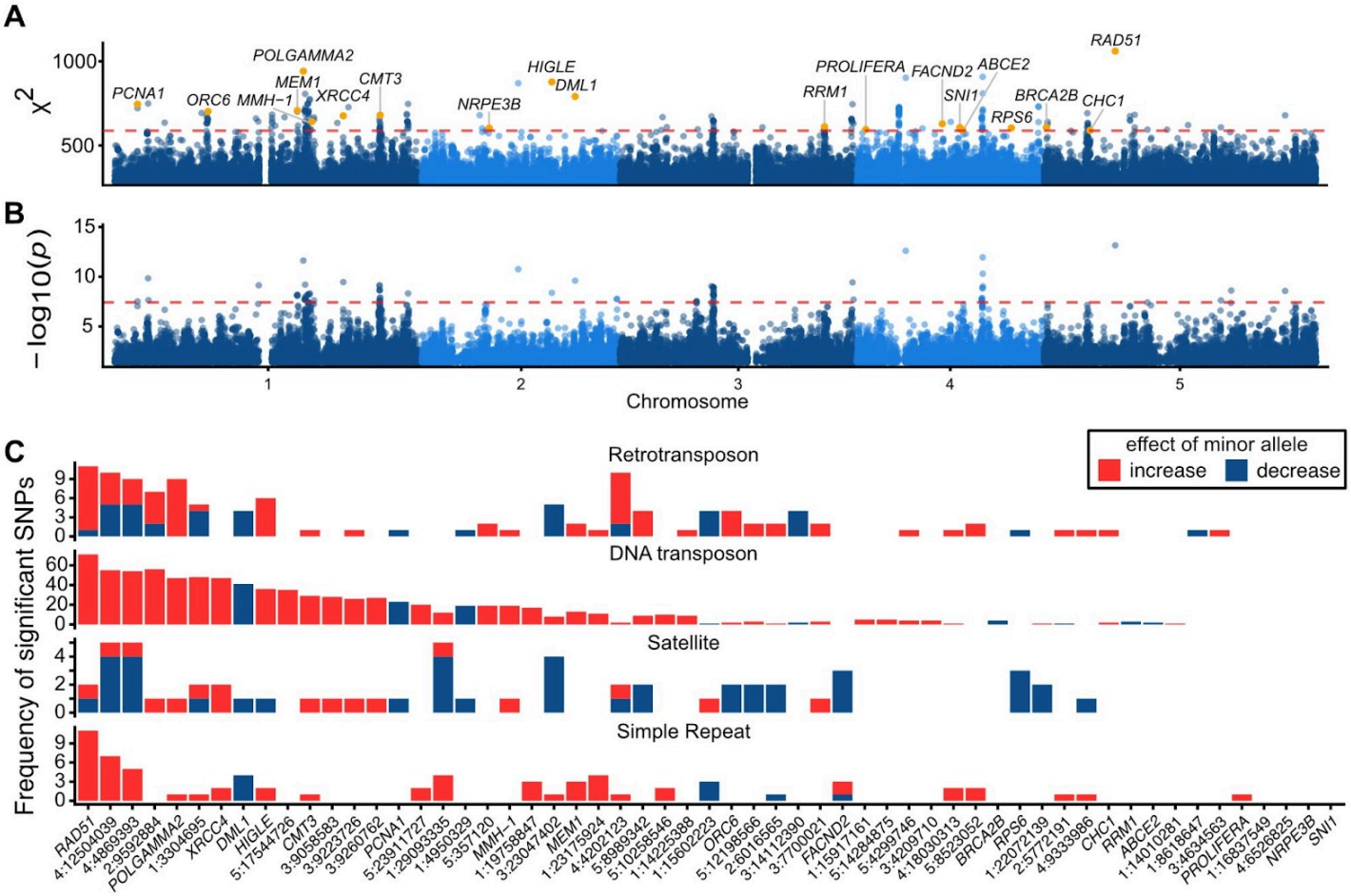

Figure 5. Genome-wide association mapping of repeat abundance.
(A) Meta-GWAS of repeat abundance. Dotted line indicates significance threshold at Bonferroni-corrected alpha = 0.05. Labels correspond to candidate genes at each locus listed in Table S6. (B) GWAS of PC 1 of repeat abundance. Dotted line indicates significance threshold at Bonferroni-corrected alpha 0.05. (C) Frequency of significant meta-GWAS tag SNPs across individual GWAS separated by sequence class. Bar colors indicate the effect of the minor allele on sequence abundance (i.e. positive beta corresponds to minor allele associated with increase in sequence copy number).

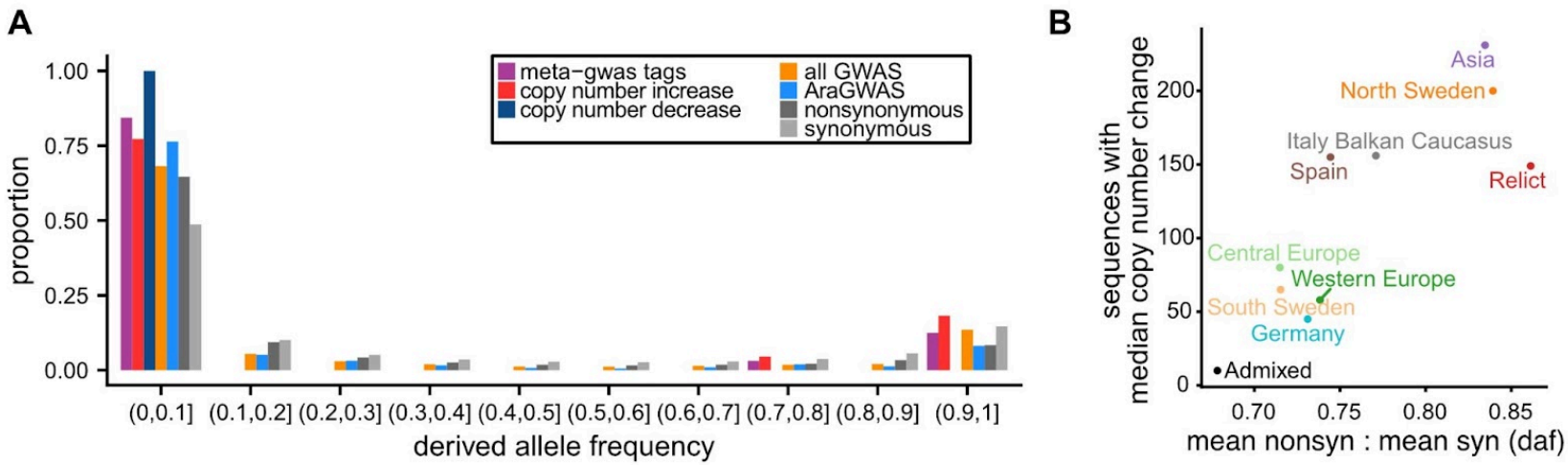

Figure 6. Evolutionary dynamics of alleles associated with copy number change.
(A) Site frequency spectra for meta-GWAS tag SNPs, meta-GWAS tag SNPs stratified by predominant copy number effect, all GWAS-associated SNPs from this study, and AraGWAS-associated SNPs, compared to nonsynonymous and synonymous SNPs from the 1001 Genomes dataset. (B) Relationship between the median number of sequences with copy number change per subpopulation (normalized to the Africa group) and the ratio of mean derived allele frequencies for nonsynonymous versus synonymous SNPs.